

HANOI UNIVERSITY OF SCIENCE AND TECHNOLOGY

GRADUATION THESIS

Performance analysis of ISAC-assisted wireless systems with energy harvesting

NGUYEN BA LINH

linh.nb203883@sis.hust.edu.vn

Embedded System and Internet of Things

Supervisor: Assoc. Prof. Nguyen Thanh Chuyen _____
Supervisor's signature

Department: Communication Engineering

HANOI, 07/2024

ĐẠI HỌC BÁCH KHOA HÀ NỘI

ĐỒ ÁN TỐT NGHIỆP

Phân tích hiệu năng hệ thống truyền tin với công nghệ truyền ISAC và mô hình thu thập năng lượng

NGUYỄN BÁ LINH

linh.nb203883@sis.hust.edu.vn

Ngành Hệ thống Nhúng và IoT

Giáo viên hướng dẫn: PGS. TS. Nguyễn Thành Chuyên

Chữ ký của GVHD

Khoa: Kỹ thuật truyền thông

Hà Nội, 07/2024

ĐÁNH GIÁ ĐỒ ÁN TỐT NGHIỆP (DÀNH CHO CÁN BỘ HƯỚNG DẪN)

Thesis title: Performance analysis of ISAC-assisted wireless systems with energy harvesting.
 Tên đề tài: Phân tích hiệu năng hệ thống truyền tin với công nghệ truyền ISAC và mô hình thu thập năng lượng.

Họ tên SV: Nguyễn Bá Linh

MSSV: 20203883

Cán bộ hướng dẫn: PSG. TS. Nguyễn Thành Chuyên

STT	Tiêu chí (Điểm tối đa)	Hướng dẫn đánh giá tiêu chí	Điểm tiêu chí
1	Thái độ làm việc (2,5 điểm)	Nghiêm túc, tích cực và chủ động trong quá trình làm ĐATN	2,5
		Hoàn thành đầy đủ và đúng tiến độ các nội dung được GVHD giao	
2	Kỹ năng viết quyển ĐATN (2 điểm)	Trình bày đúng mẫu quy định, bố cục các chương logic và hợp lý: Bảng biểu, hình ảnh rõ ràng, có tiêu đề, được đánh số thứ tự và được giải thích hay đề cập đến trong đồ án, có căn lề, dấu cách sau dấu chấm, dấu phẩy, có mở đầu chương và kết luận chương, có liệt kê tài liệu tham khảo và có trích dẫn, v.v.	2
		Kỹ năng diễn đạt, phân tích, giải thích, lập luận: Cấu trúc câu rõ ràng, văn phong khoa học, lập luận logic và có cơ sở, thuật ngữ chuyên ngành phù hợp, v.v.	
3	Nội dung và kết quả đạt được (5 điểm)	Nêu rõ tính cấp thiết, ý nghĩa khoa học và thực tiễn của đề tài, các vấn đề và các giả thuyết, phạm vi ứng dụng của đề tài. Thực hiện đầy đủ quy trình nghiên cứu: Đặt vấn đề, mục tiêu đề ra, phương pháp nghiên cứu/ giải quyết vấn đề, kết quả đạt được, đánh giá và kết luận.	5
		Nội dung và kết quả được trình bày một cách logic và hợp lý, được phân tích và đánh giá thỏa đáng. Biện luận phân tích kết quả mô phỏng/ phần mềm/ thực nghiệm, so sánh kết quả đạt được với kết quả trước đó có liên quan.	
		Chỉ rõ phù hợp giữa kết quả đạt được và mục tiêu ban đầu đề ra đồng thời cung cấp lập luận để đề xuất hướng giải quyết có thể thực hiện trong tương lai. Hàm lượng khoa học/ độ phức tạp cao, có tính mới/tính sáng tạo trong nội dung và kết quả đồ án.	
4	Điểm thành tích (1 điểm)	Có bài báo KH được đăng hoặc chấp nhận đăng/ đạt giải SV NCKH giải 3 cấp Trường trở lên/ Các giải thưởng khoa học trong nước, quốc tế từ giải 3 trở lên/ Có đăng ký bằng phát minh sáng chế. (1 điểm)	0
		Được báo cáo tại hội đồng cấp Trường trong hội nghị SV NCKH nhưng không đạt giải từ giải 3 trở lên/ Đạt giải khuyến khích trong cuộc thi khoa học trong nước, quốc tế/ Kết quả đồ án là sản phẩm ứng dụng có tính hoàn thiện cao, yêu cầu khối lượng thực hiện lớn. (0,5 điểm)	0
Điểm tổng các tiêu chí:			9,5
Điểm hướng dẫn:			9,5

Cán bộ hướng dẫn
(Ký và ghi rõ họ tên)


Nguyễn Thành Chuyên

Điểm từng tiêu chí cho lẻ đến 0,5. Nếu Điểm tổng các tiêu chí > 10 thì Điểm hướng dẫn làm tròn thành 10.

ĐÁNH GIÁ ĐỒ ÁN TỐT NGHIỆP (DÀNH CHO CÁN BỘ PHẢN BIỆN))

Thesis title: Performance analysis of ISAC-assisted wireless systems with energy harvesting.

Tên đề tài: Phân tích hiệu năng hệ thống truyền tin với công nghệ truyền ISAC và mô hình thu thập năng lượng.

Họ tên SV: Nguyễn Bá Linh

MSSV: 20203883

Cán bộ phản biện:

STT	Tiêu chí (Điểm tối đa)	Hướng dẫn đánh giá tiêu chí	Điểm tiêu chí
1	Trình bày quyển ĐATN (4 điểm)	Đồ án trình bày đúng mẫu quy định, bố cục các chương logic và hợp lý: Bảng biểu, hình ảnh rõ ràng, có tiêu đề, được đánh số thứ tự và được giải thích hay đề cập đến trong đồ án, có căn lề, dấu cách sau dấu chấm, dấu phẩy, có mở đầu chương và kết luận chương, có liệt kê tài liệu tham khảo và có trích dẫn, v.v.	
		Kỹ năng diễn đạt, phân tích, giải thích, lập luận: Cấu trúc câu rõ ràng, văn phong khoa học, lập luận logic và có cơ sở, thuật ngữ chuyên ngành phù hợp, v.v.	
2	Nội dung và kết quả đạt được (5.5 điểm)	Nêu rõ tính cấp thiết, ý nghĩa khoa học và thực tiễn của đề tài, các vấn đề và các giả thuyết, phạm vi ứng dụng của đề tài. Thực hiện đầy đủ quy trình nghiên cứu: Đặt vấn đề, mục tiêu đề ra, phương pháp nghiên cứu/ giải quyết vấn đề, kết quả đạt được, đánh giá và kết luận.	
		Nội dung và kết quả được trình bày một cách logic và hợp lý, được phân tích và đánh giá thỏa đáng. Biện luận phân tích kết quả mô phỏng/ phần mềm/ thực nghiệm, so sánh kết quả đạt được với kết quả trước đó có liên quan.	
		Chỉ rõ phù hợp giữa kết quả đạt được và mục tiêu ban đầu đề ra đồng thời cung cấp lập luận để đề xuất hướng giải quyết có thể thực hiện trong tương lai. Hàm lượng khoa học/ độ phức tạp cao, có tính mới/ tính sáng tạo trong nội dung và kết quả đồ án.	
3	Điểm thành tích (1 điểm)	Có bài báo KH được đăng hoặc chấp nhận đăng/ đạt giải SV NCKH giải 3 cấp Trường trở lên/ Các giải thưởng khoa học trong nước, quốc tế từ giải 3 trở lên/ Có đăng ký bằng phát minh sáng chế. (1 điểm)	
		Được báo cáo tại hội đồng cấp Trường trong hội nghị SV NCKH nhưng không đạt giải từ giải 3 trở lên/ Đạt giải khuyến khích trong cuộc thi khoa học trong nước, quốc tế/ Kết quả đồ án là sản phẩm ứng dụng có tính hoàn thiện cao, yêu cầu khối lượng thực hiện lớn. (0,5 điểm)	
Điểm tổng các tiêu chí:			
Điểm phản biện:			

Cán bộ phản biện
(Ký và ghi rõ họ tên)

Điểm từng tiêu chí cho lẻ đến 0,5. Nếu Điểm tổng các tiêu chí > 10 thì Điểm phản biện làm tròn thành 10.

PREFACE

Integrated Sensing and Communication (ISAC) systems represent a significant advancement in the convergence of communication and sensing technologies. By integrating sensing capabilities directly into communication infrastructure, ISAC systems can provide real-time data collection and transmission, leading to more responsive and intelligent networks.

Despite promising applications, ISAC systems face significant energy efficiency challenges. The dual sensing and communication functions demand substantial power, limiting their use in remote or resource-constrained areas. Traditional systems rely on fixed power supplies or batteries, which are unsustainable long-term due to limited lifespans and frequent replacements or recharging needs.

After SWIPT is implemented, the proposed relay-assisted ISAC system can harvest energy to power its operations, thus extending its operational lifetime and enhancing its sustainability. This approach not only mitigates the energy limitations but also improves the overall performance of the system by ensuring continuous and reliable operation.

By comprehensively analyzing the S&C performance through the derivation of exact and asymptotic formulas for key performance metrics, including the outage probability, sensing rate, and Cramer-Rao Lower Bound (CRLB) for distance estimation, I can gain valuable insights into the reliability and efficiency of the energy harvesting-enabled relay network in supporting ISAC applications.

It is important to acknowledge the significant contributions of individuals in completing this project. Assoc. Prof. Nguyen Thanh Chuyen has been an exceptional mentor and guide at the Communication Theory and Application Research Group (CTARG). His continuous support, encouragement, and logical approach to research have been invaluable throughout this journey. Secondly, I extend my heartfelt gratitude to PhD. Vu Thai Hoc, who guided and inspired me to pursue research in the field of wireless communication when I was starting from scratch.

I am deeply grateful to my family, friends, and CTARG members for their unwavering support both in material assistance and moral encouragement during my studies at Hanoi University of Science and Technology. Their support has been crucial to my personal and academic development.

Through this study, I aim to significantly contribute to the development of ISAC systems, and I am dedicated to exploring innovative solutions to improve sensing and communication performance amidst the continuously evolving technological landscape.

STATEMENT OF ORIGINALITY

I am Nguyen Ba Linh, student ID 20203883, class Embedded System and Internet of Things 02 - Cohort 65. My supervisor is Associate Professor Nguyen Thanh Chuyen from The School of Electrical and Electronics, HUST. I commit that all the information presented in this thesis "*Performance analysis of ISAC-assisted wireless systems with energy harvesting*" is the result of my study and research process. All the results stated in this document are completely honest, reflecting the actual simulation and measurement results. All references are cited following the regulations on intellectual property and listed clearly. I take full responsibility for the content written in this thesis.

Hanoi, 7th, August, 2024

Committed person

Nguyen Ba Linh

TABLE OF CONTENTS

CHAPTER 1. INTRODUCTION	1
1.1 Literature Review and Motivations	1
1.2 Contribution	3
1.3 Organization	3
CHAPTER 2. THEORETICAL BACKGROUND	4
2.1 Fundamental about ISAC system	4
2.1.1 Ideas of ISAC systems	5
2.1.2 Performance metrics of Communication	6
2.1.3 Performance metrics of Sensing	7
2.2 Relay network associated with SWIPT technique	8
2.2.1 Relay network overview	9
2.2.2 SWIPT technique	10
2.2.3 Relay meets SWIPT	13
2.3 Summary	13
CHAPTER 3. SYSTEM MODEL	15
3.1 System Description	15
3.2 Phase I: SWIPT phase	16
3.2.1 Transmitter Model	16
3.2.2 Wireless channel	18
3.3 Phase II: ISAC phase	18
3.3.1 Harvesting and Decoding	18
3.3.2 ISAC task	23
3.3.3 Sensing Information Forwarding	24
3.4 Summary	24
CHAPTER 4. PERFORMANCE ANALYSIS	26

4.1	Outage probability at Relay	26
4.2	Performance in ISAC task	27
4.3	End-to-end outage performance	30
4.4	Summary	33
CHAPTER 5. NUMERICAL RESULTS AND DISCUSSIONS		34
CONCLUSION		38

LIST OF ABBREVIATIONS

5G	Fifth-generation
ADC	Analog-to-digital
AWGN	Additive White Gaussian Noise
BS	Base station
CRLB	Cramer-Rao lower bound
DF	Decode-and-Forward
DFRC	Dual-functional radar communications
EH	Energy Harvesting
ID	Information decoding
ISAC	Integrated Sensing and Communication
ISCAP	Integrated sensing, communication, and powering
JCAS	Joint communication and sensing
JCR	Joint communications radar
JRC	Joint radar communications
LoS	Light-of-Sight
LPF	Low-pass filter
OP	Outage Probability
MD	Mobile device
MISO	Multiple Input Single Output
PDF	Probability dense function
PS	Power-splitting
RadCom	Radar-communication
S&C	Sensing and Communication
SF	Sensing-information forwarding
SNR	Signal-to-Noise ratio
SWIPT	Simultaneous wireless information and power transfer
TIR	Target impulse response

LIST OF FIGURES

Figure 1.1	Scenario of the application of ISAC-aided by relay network in the disaster recovery services	2
Figure 2.1	Some application scenarios of ISAC in the future, [1]	4
Figure 2.2	The overview of classifications of ISAC, [2]	6
Figure 2.3	Relaying network	10
Figure 2.4	Advantages and limitations of various receiver schemes of SWIPT	12
Figure 3.1	WPT-powered ISAC transmission model.	15
Figure 3.2	Power Splitting Relaying protocol at ISAC phase.	16
Figure 3.3	The illustration of the simplified transmit diversity model.	17
Figure 3.4	Rectenna equivalent circuit [3]	19
Figure 3.5	Coherent demodulation at R_X equivalent scheme [4]	20
Figure 3.6	Power splitting scheme for receiver	21
Figure 5.1	Outage probability at Relay, as a function of the transmit power at BS with fixed value $\rho = 0.3$	35
Figure 5.2	Outage probability at Relay as a function of the transmit power at BS and the power splitting ratio ρ	35
Figure 5.3	The outage probability for source information decoding at MD as a function of the transmit power at BS with fixed value $\rho = 0.3$	36
Figure 5.4	The end-to-end outage probability at MD as a function of the transmit power at BS with fixed value $\rho = 0.3$	36
Figure 5.5	The sensing rate in ISAC task as a function of the transmit power at BS with fixed value $\rho = 0.3$	37

LIST OF TABLES

Table 2.1	Advantages & limitations of various types of relaying.	11
Table 4.1	Self-defined constants and functions.	26
Table 5.1	Simulation Parameters	34

TÓM TẮT ĐỒ ÁN

Hệ thống 5G-Advanced (5G-A) và các công nghệ sau này được kỳ vọng sẽ đóng vai trò quan trọng trong việc hiện thực hóa nhiều ứng dụng mới nổi, với công nghệ tích hợp cảm biến và truyền thông (ISAC) là một trong những công nghệ nổi bật và đầy hứa hẹn [1,5]. ISAC giới thiệu khả năng cảm biến vô tuyến vào các hệ thống truyền thông di động truyền thống và hiện đại. Với sự phát triển của các mảng ăng-ten lớn hơn và băng tần số rộng hơn để nâng cao năng lực truyền thông, các hệ thống này sẽ hưởng lợi đáng kể từ việc cảm biến vô tuyến [6–9]. Do đó, việc tích hợp truyền thông và cảm biến đang nổi lên như một công nghệ đầy hứa hẹn, tận dụng những tiến bộ trong các hệ thống truyền thông.

Tuy nhiên, hệ thống ISAC phải đối mặt với thách thức về hạn chế năng lượng, có thể làm giảm hiệu suất và gây ra sự không ổn định [10, 11]. Để giảm thiểu những hạn chế về năng lượng này, tôi đề xuất một sơ đồ thu hoạch năng lượng tại trạm chuyển tiếp nhằm tăng cường hiệu quả và độ tin cậy của hệ thống ISAC. Phương pháp của tôi bao gồm việc đánh giá việc tích hợp các kỹ thuật thu hoạch năng lượng vào trạm chuyển tiếp, từ đó cho phép hoạt động bền vững và cải thiện hiệu suất tổng thể của hệ thống. Tôi tiến hành phân tích xác suất dừng toàn diện, xem xét các thông số chính như xác suất ngừng hoạt động từ đầu đến cuối và tốc độ cảm biến.

Kết quả cho thấy rằng sơ đồ đề xuất cải thiện đáng kể hiệu quả và độ tin cậy của hệ thống. Các xác nhận lý thuyết thêm vào chứng minh tính khả thi của những phát triển của chúng tôi, làm nổi bật những lợi ích thực tế của phương pháp thu hoạch năng lượng trong việc nâng cao hiệu suất hệ thống ISAC. Luận văn này đóng góp vào lĩnh vực bằng cách đưa ra một giải pháp khả thi cho các hạn chế về năng lượng của các hệ thống ISAC, mở đường cho các ứng dụng truyền thông và cảm biến không dây mạnh mẽ và bền vững hơn.

ABSTRACT

5G-Advanced (5G-A) and beyond are anticipated to be crucial for enabling numerous emerging applications, with integrated sensing and communications (ISAC) technology being one of the most distinctive and promising [1, 5]. It introduces radio sensing capabilities into traditional and modern mobile communication systems. With the evolution towards larger antenna arrays and broader frequency bandwidths to enhance communication capacity, these systems are poised to significantly benefit radio sensing [6–9]. As a result, integrating communication and sensing is emerging as a promising technology, leveraging advancements in communication systems.

However, the ISAC system faces the challenge of limited energy, which can restrict performance and cause instability [10, 11]. To mitigate the energy limitations, I propose a relay energy harvesting scheme designed to enhance the efficiency and reliability of the ISAC system. Our approach involves evaluating the integration of energy harvesting techniques into the relay, thereby enabling sustainable operation and improving overall system performance. I conduct a comprehensive performance analysis, examining key metrics such as end-to-end outage probability and sensing rate.

The results demonstrate that the proposed scheme significantly improves the system's efficiency and reliability. Numerical validations further support our findings, highlighting the practical advantages of the energy harvesting approach in enhancing ISAC system performance. This thesis contributes to the field by offering a viable solution to the energy constraints of ISAC systems, paving the way for more robust and sustainable wireless communication and sensing applications.

CHAPTER 1. INTRODUCTION

1.1 Literature Review and Motivations

Integrated sensing and communication (ISAC) systems, through the sharing of spectrum and hardware resources, are capable of providing not only high-quality wireless connections but also superior sensing resolution and accuracy. These capabilities will be crucial for the development of future Internet of Things (IoT) systems [7]. ISAC is well-suited for numerous environmental sensing applications, including virtual reality, smart factories, healthcare, and intelligent transportation. Consequently, research on ISAC has garnered significant attention from both industry and academia in recent years. In [12], the researchers examined a millimeter-wave ISAC system and demonstrated its ability to achieve mutual benefits for both sensing and communication functions by effectively utilizing shared common information. In [13], the researchers explored a co-operative ISAC network, where a micro base station (BS) can function both as a sensing device and a full-duplex decoding forwarding relay. However, a significant issue in many ISAC scenarios is the limited energy, which can restrict performance and lead to instability. In addition in the future, the ISAC model will be embedded into IoT devices (low-power devices), especially wireless devices. They will have to be charged to support the sustainable operation of massive IoT devices. Compared to physical wired charging, wireless charging is more convenient by reducing the hassle of connecting cables, more cost-effective by enabling on-demand energy supplies and uninterrupted operations, and sometimes essential for applications in which manual battery replacement/recharging is dangerous (e.g., in the radioactive area) or even impossible (e.g., for biomedical implants). Several wireless power transfer (WPT) technologies have been developed to facilitate wireless charging, including electromagnetic induction, magnetic resonance, and RF power transmission [14]. However, for far-field wireless communication, WPT using RF is suitable for longer distances. Additionally, there is an interesting reason that the RF waves can simultaneously carry both information and energy, which is known as Simultaneous wireless information and power transfer (SWIPT) [3]. In SWIPT, the Energy Receivers (ER) and the Information Receivers (IR) can either be co-located or separated. When the receivers are separated, the ER and IR are distinct devices: the ER is a low-power device being charged, while the IR is a device receiving data. In contrast, with co-located receivers, each receiver is a single low-power device that is simultaneously charged and receives data. Given the capabilities of SWIPT to deliver both energy and information, it becomes evident that integrating SWIPT with relay networks (which have limited battery lifetime and so their life cycle depends on the life cycle of the battery) could offer significant advantages. This integration enables the relay to use the

harvested energy for information forwarding, mitigating the impacts of fading, path loss, shadowing, limited coverage, and low signal-to-noise ratio (SNR), thereby improving the overall performance of the communication system.

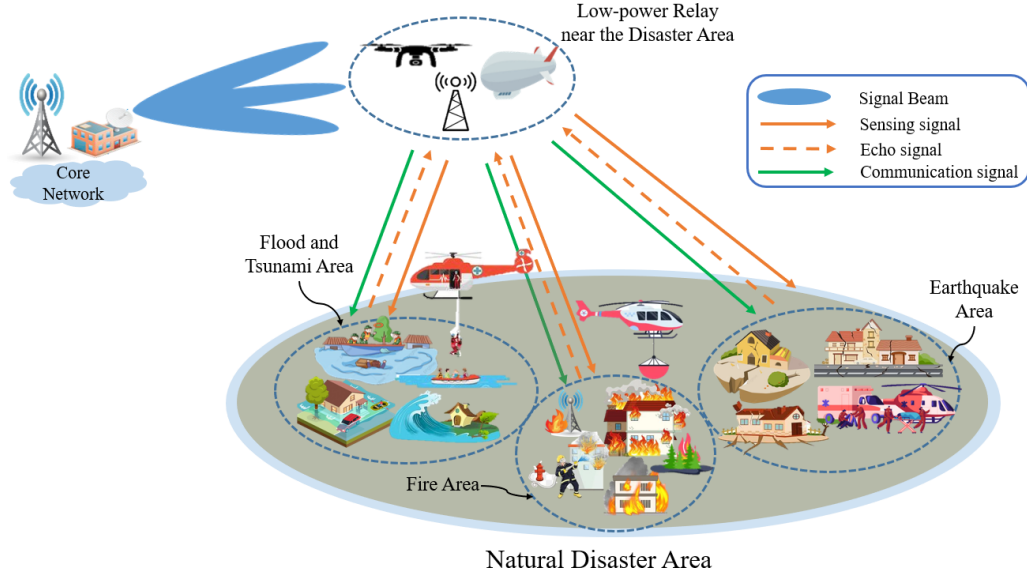


Figure 1.1 Scenario of the application of ISAC-aided by relay network in the disaster recovery services

To the best of my knowledge, there has been limited research investigating ISAC aided by energy harvesting-enabled relay networks. In [15], the author proposed multi-functional wireless systems that can provide sensing, communication, and powering (ISCAP) capabilities simultaneously. Additionally, [16] introduced a WPT model for ISAC edge devices. However, these models do not highlight the strength of the relay network. In other words, the communication range between the UE and the central unit is limited. Motivated by this observation, this thesis aims to propose a relay network in which the relay is a low-power ISAC system capable of utilizing the energy provided by a source to forward both the source's information and the sensed target information to the user. It is crucial to evaluate the S&C performance by deriving their respective formulas. To be practical, I will consider a scenario that involves a service for remote disaster recovery and management as depicted in Figure 1.1. In the remote areas affected by natural disasters (e.g. earthquakes, floods, tsunamis,...), the traditional communication infrastructure has been severely damaged, making it difficult for rescue teams to coordinate and manage recovery operations effectively. Specifically, a conventional rescue system may consist of a portable or mobile BS deployed near the disaster area to provide a communication backbone, a low-power relay is located strategically throughout the disaster zone, positioned where it not only has a good line of sight (LoS) with the BS but also suffers the least damage from disasters, a MD carried by rescue team, require to maintain the strong and stable connection for communication and coordination with BS. In this

scenario, due to the dangerous conditions area, R cannot be charged normally (e.g., replacing batteries, power supply via wires) so it can take advantage of BS's EM radiation to harvest energy. Also in the same area, MD may not have a good link with the BS (e.g. the direct link is extreme shadowing due to obstructions like debris or collapsed structures), so they need to use R to forward the BS information for MD. Moreover, the rescue team needs to locate survivors (e.g. trapped under rubble or underwater), especially in low light or hostile environments. Hence, the radar sensing by relay ISAC capability allows rescue teams to pinpoint the locations, for example, through echo signal, the relay estimates the distance from survivors and embeds this info to the BS information before forwarding it to MD, facilitating timely rescue efforts.

1.2 Contribution

The primary objective of this thesis is to conduct a comprehensive performance analysis of ISAC-assisted wireless systems with energy harvesting. This involves evaluating the impact of integrating relay energy harvesting techniques into ISAC systems to enhance the overall efficiency and reliability of wireless communications and sensing tasks. The major contributions of this thesis are summarized as follows:

- **C1:** Proposal of a relay energy harvesting scheme for the ISAC-assisted system, aimed at improving its efficiency and reliability.
- **C2:** Development of a detailed performance analysis of the system, encompassing metrics such as end-to-end outage probability and sensing performance metrics.
- **C3:** Presentation of numerical results to validate the proposed analysis and demonstrate the practical benefits of the scheme.

1.3 Organization

The remainder of this thesis is organized as follows: Chapter 2 delves into the background of Integrated Sensing and Communication (ISAC) systems, providing a comprehensive overview of the fundamental concepts, and key performance metrics in this field. The system model is detailed in Chapter 3. Chapter 4 presents an in-depth performance analysis, discussing the metrics used and the theoretical foundations of the analysis. The simulation results to validate the theoretical development, followed by a thorough discussion are given in Chapter 5 and finally concludes the thesis.

CHAPTER 2. THEORETICAL BACKGROUND

2.1 Fundamental about ISAC system

Over the past few decades, wireless communications and radar systems have advanced in parallel. Wireless technology has evolved from first-generation (1G) to fifth-generation (5G) networks, while radar systems have progressed from basic target detection and range estimation to sophisticated sensing capabilities like tracking, imaging, and classification. The integrated sensing and communication known as ISAC, has recently attracted considerable interest from both academia and industry, particularly in the context of beyond 5G and sixth-generation (6G) mobile communication systems. With the development and application of millimeter-wave (mmWave) and terahertz (THz) technologies, the frequency bands of communication gradually coincide with these of radar, which promotes the realization of ISAC technology [17]. This integration holds the

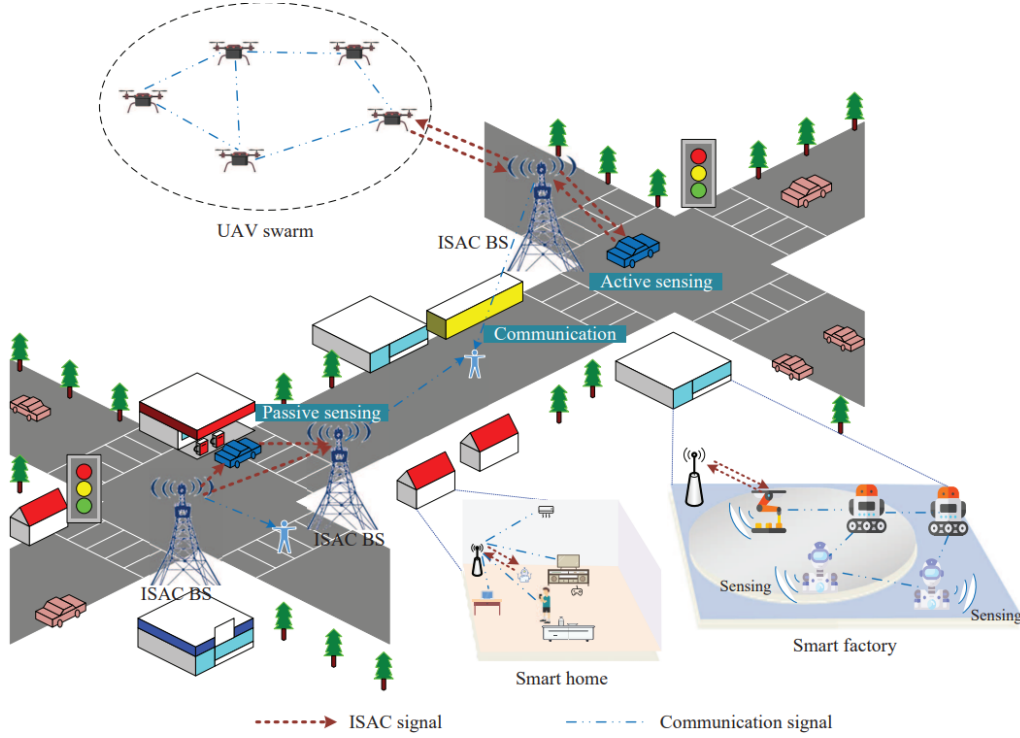


Figure 2.1 Some application scenarios of ISAC in the future, [1]

potential to support a variety of future applications, such as remote industrial management, weather monitoring, asset tracking, smart homes, and autonomous vehicles, as illustrated in Figure 2.1.

2.1.1 *Ideas of ISAC systems*

The concept of ISAC emerged in the last century. Initially, radar and communication systems were developed independently. However, the evolution of 5G technology has driven these systems towards integration. In the 1860s, Mealey et al. [18] pioneered the combination of communication and radar sensing technologies over a missile range instrumentation radar via pulse interval modulation (PIM), where information was embedded into a group of radar pulses. The first ISAC scheme using chirp signals was introduced by the authors of [19], where combining chirp signals with PSK modulations. Liu et al. [1, 7, 20] provided a comprehensive review of ISAC's development in recent years, outlining the transition from independently evolving radar and communication systems to their gradual integration, culminating in the realization of ISAC. Their article [7] provides a detailed overview of the history of ISAC. The idea of ISAC is to combine the functionalities of sensing and communication within a single system, utilizing shared wireless resources to perform both tasks efficiently [7]. This dual-functionality approach leverages advancements in wireless technology to create a cohesive system that can simultaneously sense the environment and communicate data. By integrating these functionalities, ISAC enhances the performance of both sensing and communication, leading to more robust and efficient systems. ISAC systems can be divided into two categories according to their sensing functionality. Each category can operate under various channel topologies, as depicted in Figure 2.2, [2]. In this context, Device-free ISAC means that within the integrated system, the sensing functionality is achieved through device-free sensing. This means the sensing targets (e.g., a bird), which are not capable of transmitting and/or receiving the sensing signal, enable the sensing functionality. A typical example of device-free sensing is radar sensing. On the other hand, the Device-based ISAC involves systems where sensing is achieved through targets that can transmit and/or receive sensing signals. Wireless-based localization, used to pinpoint mobile devices, is a typical example of device-based sensing.

Despite extensive research on ISAC, numerous crucial elements remain insufficiently examined, including the formulation of a unified analytical framework, the determination of theoretical performance boundaries, and the development of optimal signal processing algorithms [21]. In recent years, a growing number of papers published on the ISAC theme generally fall into two primary categories: analysis of Sensing and Communication (S&C) performance [2], and dual-functional beamforming design [22]. Within these two topics, many S&C performance metrics have been proposed. In the following section, I will introduce some basic S&C performance metrics at the PHY layer. From there, I will also select the performance metrics to focus on for this thesis.

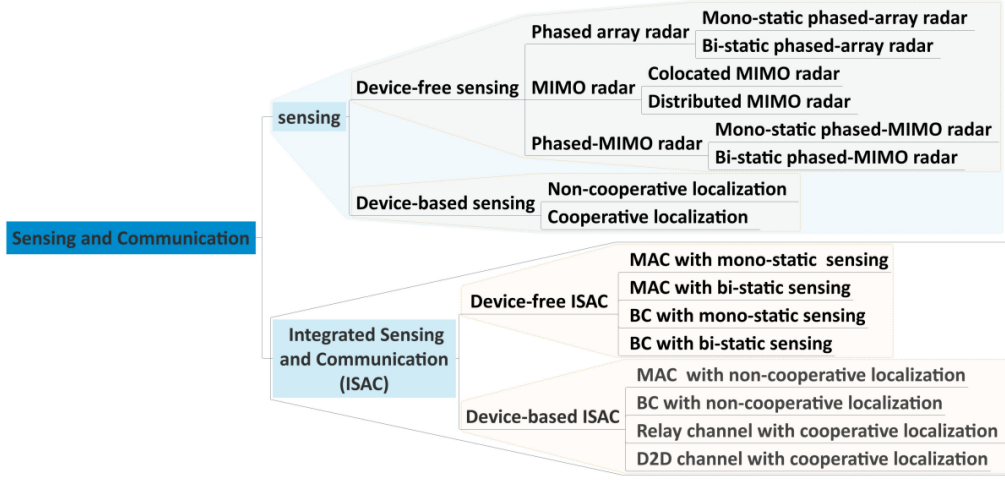


Figure 2.2 The overview of classifications of ISAC, [2]

2.1.2 Performance metrics of Communication

In general, communication performance can be evaluated from two aspects, i.e., efficiency and reliability, with the following definitions:

- **Efficiency:** Effectively transmitting information necessitates the use of wireless resources, including spectrum, spatial, and energy resources. Therefore, efficiency serves as a measure of how much information is successfully conveyed from the transmitter to the receiver, within the constraints of the available resources [23, 24]. Spectral efficiency and energy efficiency are commonly used metrics, characterized by the achievable rate per unit of bandwidth or energy, measured in bit/s/Hz or bits per channel use, and bit/s/Joule, respectively. Additionally, channel capacity, coverage area, and the maximum number of users that can be served are crucial factors for evaluating efficiency.
- **Reliability:** A communication system should have resilience towards harmful factors within the communication channel. In other words, we expect the communication system to operate in the presence of noise, interference, and fading effects. Accordingly, reliability measures the ability of a communication system to reduce or even correct erroneous information bits [23], [24]. Commonly used metrics include outage probability (OP), bit error rate (BER), symbol error rate (SER), and frame error rate (FER).

In this thesis, the key performance metric I have focused on is the OP. The OP, normally denoted by \mathcal{P}_{out} , is a crucial parameter for evaluating the reliability of the communication system. Physically, this indicator represents the probability that the achieved rate \mathcal{R} at the receiver for decoding the transmitted signal falls below a required threshold, denoted

by \mathcal{R}^{th} . This event makes it difficult for the receiver to detect the original information. Mathematically, the outage probability can be calculated by [25]:

$$\mathcal{P}_{out} = \Pr(\mathcal{R} < \mathcal{R}^{th}) = F_X(\gamma^{th}) = \int_0^{\gamma^{th}} f_X(x) dx,$$

where $F_X(x)$ and $f_X(x)$ denote the CDF and PDF of channel coefficient or instantaneous SNR, γ^{th} is the SNR threshold, which has derived from the rate threshold \mathcal{R}^{th} by the Shannon theorem [25]:

$$\mathcal{R}^{th} = \log_2(1 + \gamma^{th}). \quad (2.1)$$

2.1.3 Performance metrics of Sensing

Sensing tasks can generally be divided into three categories: detection, estimation, and recognition, all of which are based on collecting signals/data related to the sensed objects [26]. Although these terms may have different meanings depending on the context and can be executed at various layers, I attempt to define them as follows:

- **Detection:** Detection refers to making binary/multiple decisions on the state of a sensed object, given the noisy and/or interfered observations. These states usually include whether a target is present or absent (PHY) and whether an event occurs (application layer), such as motion detection. This process can be represented as a binary or multi-hypothesis testing problem. For instance, in a binary detection scenario, I select between two hypotheses, \mathcal{H}_1 and \mathcal{H}_0 , such as the target being present or absent, based on the observed signals. Metrics for detection include the detection probability, which is the probability that \mathcal{H}_1 is true and the detector selects \mathcal{H}_1 , and the false-alarm probability, which is the probability that \mathcal{H}_0 is true but the detector selects \mathcal{H}_1 [27]. In the context of ISAC, several articles have focused on this key performance indicator [28, 29].
- **Estimation:** Estimation involves extracting valuable parameters of the sensed object from noisy and/or interfered observations. This process may include estimating the distance, velocity, angle, quantity, or size of the target(s). Estimation performance is typically evaluated using the mean squared error (MSE) and the Cramer-Rao Lower Bound (CRLB) [25]. MSE is defined as the average of the squared errors between the actual value of a parameter θ and its estimated value $\hat{\theta}$. CRLB represents the lower bound on the variance of any unbiased estimator for θ , calculated as the inverse of the Fisher Information (FI). FI is the expected value of the curvature (negative second derivative) of the likelihood function with respect to θ , indicating the "sharpness" or precision of the estimator.
- **Recognition:** Recognition refers to understanding *what* the sensed object is based on noisy and/or interfered observations. This process may include recognizing

targets or identifying human activities/events. Recognition is usually considered a classification task at the application layer, with performance measured by recognition accuracy [30].

For sensing tasks over PHY, detection probability and CRLB are of particular interest [1, 29]. For higher-layer applications, recognition accuracy is at the core of learning-based schemes. More advanced sensing tasks, e.g., imaging, require multiple detection and estimation operations to be performed over a complex target.

In this thesis, I have selected the suitable sensing service for the scenarios outlined. The estimation of the distance between the relay and the survivor will be used, and the CRLB is the performance metric used to analyze it. Furthermore, from an information-theoretic perspective, I will use the sensing rate (SR) for sensing performance analysis. The SR is defined as the sensing mutual information (MI) per unit, it tells how much information we can extract from the nearby environment from an information-theoretical point of view based on the echo signal. This metric is a new parameter that has been selected by many recent papers [31–33].

2.2 Relay network associated with SWIPT technique

As an established method [34, 35], relaying networks are extensively employed in modern wireless communication systems to effectively increase data rates within a specific area, and boost spectrum efficiency without the additional construction of base stations, which could lead to substantial hardware and administrative expenses. Also, communication relaying technology minimizes path-loss and fading effects efficiently, thereby resulting in an increased coverage area and capacity of the system. This method is particularly advantageous because it leverages existing infrastructure to improve performance, thereby reducing the need for costly new installations. In the upcoming generation of wireless communication, the adoption of higher frequency spectrums is expected to enhance data transmission capabilities significantly. However, this shift also presents challenges, notably more pronounced signal attenuation due to the physical properties of higher frequency waves. To address this issue and ensure that users receive sufficiently strong signals, the deployment of small cells will be necessary in future networks. These small cells will act as supplementary nodes to fill coverage gaps and support increased access, thereby ensuring a robust and reliable network. Consequently, cost-effective and energy-efficient solutions for 5G technology are critically needed to meet the growing demand for high-speed, high-capacity wireless communication. Up to now, relaying networks have been identified as a crucial component in the next generation of wireless communication, playing a pivotal role in the development and deployment of 5G& beyond networks. However, relay nodes are typically battery-constrained or even battery-less devices, which necessitates the need for external charging systems.

Replacing or recharging the batteries of these devices is often neither feasible nor convenient, especially in remote or inaccessible locations. Consequently, energy harvesting (EH) has emerged as a highly cost-effective, suitable, and safer solution to power these relays. EH techniques can convert ambient energy from various sources such as solar, thermal, or radio frequency into electrical power, which can be used to energize the relay nodes. Among the various types of energy harvesting techniques, SWIPT stands out as the most prominent. SWIPT is particularly advantageous because it provides spectral efficiency by simultaneously delivering both energy and information to the relay nodes. This dual-functionality not only optimizes the use of the available spectrum but also ensures that the relay nodes remain operational without the constant need for battery replacements or recharges.

2.2.1 Relay network overview

The concept of the relay was first introduced in [36]. Here, the authors considered a three-node communication (source-relay-destination). Relay nodes function as intermediaries [37], forwarding packets from the source node to the destination node in a multi-hop wireless communication network. This allows devices that are beyond the range of BS to still establish communication with these points. An example of how a wireless relay network is applied is usually depicted in Figure 2.3. In such a scenario, the source signal can be transmitted directly to the destination when feasible, or alternatively, through a relay node. If direct transmission to the destination is not possible, for example, due to a poor direct link caused by obstacles or severe fading, a relay node becomes essential. Initially, the source sends its packets to the relay node. The relay node then forwards the data to the destination after applying cooperative relaying mechanisms.

Relaying systems can be classified into two main categories:

- Fixed relaying: The relay node operates in active mode, with resources between the source and relay allocated in a deterministic manner, which leads to spectral inefficiency.
- Adaptive relaying: the relay node activates only when it needs to process information; otherwise, it stays silent or inactive, enhancing spectral efficiency and reliability. Nevertheless, this method demands higher computational power and may introduce some delays [38].

In the type of Fixed relaying, is separated into three types of relaying mechanisms: **Amplify-and-Forward Relaying:** In this scheme, the relay amplifies the received signal from the source and then forwards the amplified signal toward the destination.

Decode-and-Forward Relaying: In this scheme, the relay node decodes the signal re-

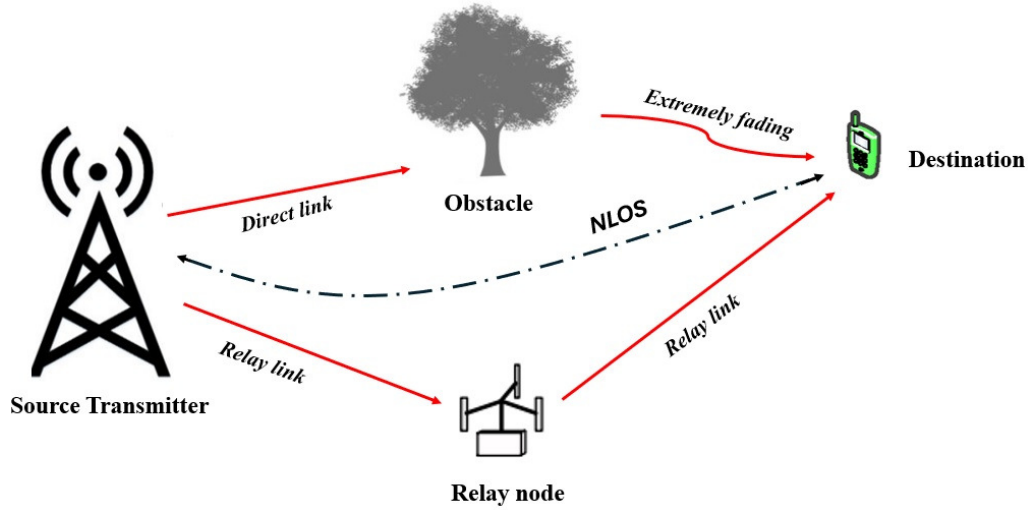


Figure 2.3 Relaying network

ceived from the source, re-encodes it, and then transmits it to the destination.

Compress-and-Forward Relaying: In this scheme, the relay node does not decode and encode the signal like in DF. Instead, it compresses the received signal from the source and forwards the compressed signal to the destination.

In the type of Adaptive relaying, is typically separated into two types of relaying mechanisms:

Selective Decode-and-Forward Relaying: In this scheme, the relay decodes messages from the source, and after performing an error check, it forwards to the destination only if correct decoding takes place; otherwise, it remains silent.

Incremental Relaying: If the direct transmission between a sender and a receiver is error-free, the relay node remains silent. But if the error is found (based on the SNR value), the relay node relays the message to the destination.

Table 2.1 below shows the summary of the advantages and drawbacks of various relaying techniques.

In this thesis, to comprehensively analyze the outage performance of the whole system, including the relay's decoding of the source message, and for simplicity, I will employ the DF relaying mechanism.

2.2.2 SWIPT technique

Wireless devices with energy constraints are often powered by batteries that have a limited lifespan. Although replacing or recharging the batteries of wireless devices can maintain normal network operations, it can lead to high operational costs or may not be feasible in certain situations. With billions of IoT devices, many batteries are needed, and they must be properly maintained and disposed of. Furthermore, the global

Types of relaying	Advantages	Performance metrics enhanced	Limitations	References
AF	A simpler form of relaying with lower processing and hardware cost. No decoding or quantizing operation is needed to perform.	Least delay.	It also amplifies the residual noise. Degrades the QoS of the network. Hard to implement in TDMA systems.	[39–41]
DF	Eliminates the noise.	Lower error rate.	Computational delay & complex. Error propagation problems might arise	[42–44]
CF	Reduce the data load by compressing.	Better throughput. Low bit error rate.	Need direct path between source and destination. Computational cost is higher	[45, 46]
S-DF	Relaying only the errorless message. Eliminates the noise.	Lower bit error rate. Higher spectral efficiency.	Increased delay. Security vulnerability.	[47]
Incremental	Error-free or errorless. Easy to implement and no need for CSI.	Higher spectral efficiency.	Higher signaling efforts. Higher system complexity.	[48, 49]

Table 2.1 Advantages & limitations of various types of relaying.

electric power consumption by the information and communications technology industry was 910 TWh in 2020, and it is forecasted to grow to 1250 TWh by 2030 [50]. It is also estimated that the annual carbon emissions will reach up to 830 Mto by 2030 [50]. This alarming situation has posed significant challenges for researchers to reduce energy consumption and carbon emissions. The proliferation of millions and billions of devices will necessitate an equally vast number of batteries. These batteries must be properly maintained and disposed of to ensure the ecosystem's health. SWIPT, a technique for energy harvesting (EH), allows simultaneous transmission of power and data [51]. The theoretical foundation of SWIPT was first proposed by Varshney [52]. While it is theoretically possible to extract both energy and information from the same waveform, practical implementation is hindered by circuit design limitations, including the different power sensitivities of receiver antennas. For instance, energy harvesting necessitates a

power sensitivity of -10 dBm, while information decoding demands a significantly lower sensitivity of -60 dBm [53]. To facilitate SWIPT, the signal must be divided into two segments: one dedicated to energy harvesting and the other to information decoding. In this thesis, I only focus on the co-located architecture receiver of EH and ID. With the co-located architecture, there are a few structures available for SWIPT as follows [54]:

Time Switching (TS): Refers to co-located receiver architecture, the same antenna is employed for EH and ID. A switch is employed at the receiver to switch between EH and ID in each time slot. This time-switching (TS) receiver requires accurate scheduling of information and energy, precise time synchronization, and benefits from hardware simplicity [54].

Power Splitting (PS): A power splitter is set up to split the received wireless signal into two streams with different power levels, one for ID and the other for energy harvesting EH [55]. The EH and ID processes are implemented simultaneously.

Antenna Switching (AS): EH and ID are employed by separate and independent antennas that can detect different channels [56]. This scheme is also known as the Space Switching scheme. It can be thought of as a distinct case for PS architecture, i.e., performing EH and ID concurrently.

The table in the figure 2.4 below shows the advantages and limitations of various SWIPT architectures

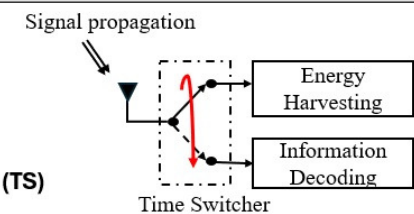
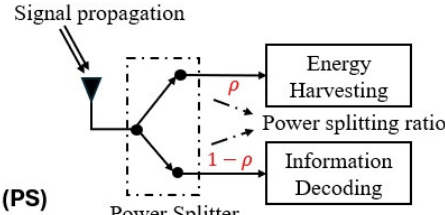
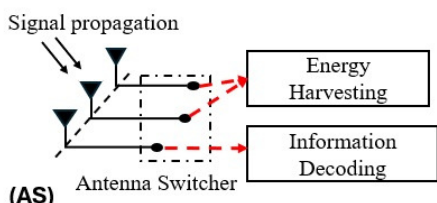
SWIPT receiver scheme	Advantages	Limitations
<p>Signal propagation</p>  <p>(TS) Time Switcher</p>	<ul style="list-style-type: none"> Simple hardware implementation. 	<ul style="list-style-type: none"> Faces synchronizarion problem. Needs proper schedule. Delay occurs
<p>Signal propagation</p>  <p>(PS) Power Splitter</p>	<ul style="list-style-type: none"> Instant ID and EH. Less susceptible to delay. 	<ul style="list-style-type: none"> More complex than TS. Needs proper optimization of the PS factor: ρ.
<p>Signal propagation</p>  <p>(AS) Antenna Switcher</p>	<ul style="list-style-type: none"> Performing both EH and ID simultaneously. 	<ul style="list-style-type: none"> Needs multiple antennas. Susceptible to optimization errorr.

Figure 2.4 Advantages and limitations of various receiver schemes of SWIPT

2.2.3 Relay meets SWIPT

Relay nodes are generally either battery-constrained, with limited battery lifetimes, or entirely battery-less, meaning their operational lifespan is directly tied to the battery's life cycle. The act of relaying data consumes energy, causing the batteries of relay nodes to deplete faster than those of non-relaying nodes. In many scenarios, such as with sensors implanted in the human body, devices embedded in walls, or nodes situated in hazardous environments, recharging or replacing batteries is both costly and impractical. To address these challenges, radio frequency (RF) energy harvesting (EH) [57] allows relay nodes to convert wireless signals from a BS into electrical power, thereby augmenting the nodes' battery life. Since a single signal is used for both functions, the SWIPT technique allows the relay nodes to decode data and recharge batteries using the same wireless signal. In a SWIPT-based relay network, relay nodes can leverage to harvest sufficient energy to transmit information from other nodes. The energy used by the relay nodes is replenished by the wireless power provided by the SWIPT-enabled (BS). There are two frameworks for the operation of a relay aided by SWIPT in the relay network. Both will be described below with consideration of a three-node relay network, Source-Relay-Destination in the total of two time slots corresponding to the time duration for transmission from Source to Relay and the time duration for forwarding from Relay to Destination, respectively.

Time-switching protocol: At the relay, the first time slot is divided into two sub-time slots: one for EH and one for ID. Subsequently, by the energy harvested previous time slot, the relay forwards the information to the destination during the remaining time slot [58].

Power-splitting protocol: At the relay, in the first time slot, the received signal from the source is split into two power streams with the ratio of ρ for example for EH and $(1 - \rho)$ for ID. Here, EH and ID are done simultaneously. Then, by the energy harvested previous time slot, the relay forwards the information to the destination during the remaining time slot [59].

In this thesis, to facilitate future analysis, I will use the power-splitting protocol with the specified power-splitting ratio ρ .

2.3 Summary

This chapter presented the theoretical background of the ISAC system and the relay networks charging by SWIPT protocol. The idea of ISAC, combines communication and sensing functionalities, leveraging shared resources to enhance efficiency and enable diverse applications. Thus, ISAC enhances spectral efficiency, reduces hardware costs, and enables predictive beamforming. Challenges such as interference management, standardization, and security are also addressed to ensure the robustness and effectiveness

of ISAC systems in future wireless networks. In the other side, relay networks enhance wireless communication by using relay nodes to forward data between source and destination, especially when direct transmission is impractical. However, these relay nodes often face energy constraints due to their reliance on batteries. SWIPT addresses this issue by enabling relay nodes to harvest energy from the same wireless signals used for data transmission. This dual-functionality not only improves the spectral efficiency of the network but also ensures that relay nodes remain powered without frequent battery replacements, making SWIPT a cost-effective and sustainable solution for powering relay networks.

CHAPTER 3. SYSTEM MODEL

Chapter 3 of this thesis delves into the development of a comprehensive system model for the relay ISAC under study. It provides a detailed introduction to the fundamental equations and parameters governing the system, breaking down the operational mechanics and interactions within each orthogonal time slot to offer a thorough understanding of the underlying processes.

3.1 System Description

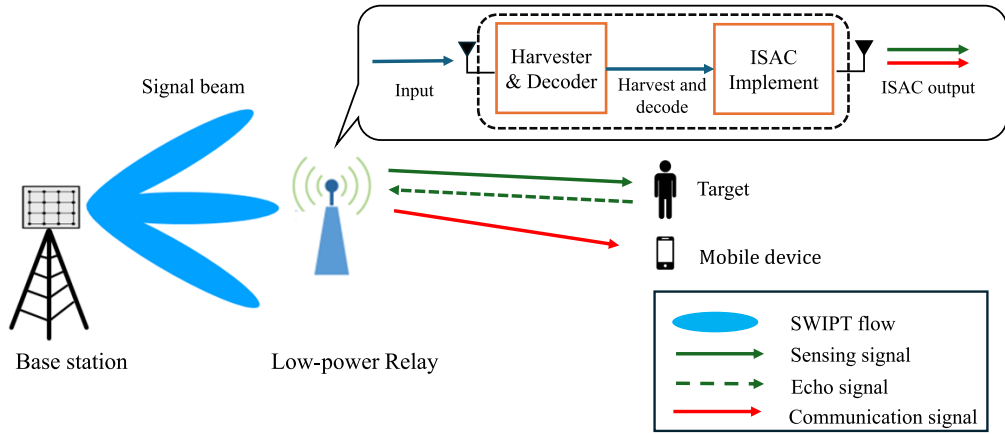


Figure 3.1 WPT-powered ISAC transmission model.

Figure 3.1 shows the proposed model, where the Base station (BS) is in charge of downlink communication with a single Mobile Device (MD). Unfortunately, the direct link between the BS and MD is awful (e.g. an obstacle in the direct link causes extreme shadowing,...) resulting in the MD being unable to receive the direct signal from the BS. Assume that a low-power device (R) has a good channel with the BS, so it can serve as a relay for end-to-end communication between BS and MD by forwarding the source signal from BS to MD. Although R functions as an ISAC equipment, it has limited power. Thereby, it could be potential to harvest energy from the BS's EM to perform both monostatic radar sensing for desired target estimation and forward the relay signal to the MD. MD has a demand for information about the sensing target as well as information from BS. Besides, it is assumed that BS is equipped with N_p antennas. R has a transmit antenna and a receive one denoted by T_X and R_X , respectively, while MD has a single antenna. The overall operation of the system consists of two orthogonal phases:

- SWIPT-phase: the BS transmits the downlink source signal (for MD) to R.
- ISAC-phase: This phase is viewed as three sub-phases:

Harvesting and Decoding : In this sub-phase, R implements the power-splitting (PS) method for energy harvesting. In particular, R harvests a fraction of the received signal power while using the remaining one for information decoding. This sub-phase takes the duration of τ_r .

ISAC task : R simultaneously conducts the sensing and communication tasks by simultaneously performing estimation sensing service on a target object located in the far field (e.g., a ... based on the echoes) and forwarding the decoded source information to the MD. This sub-phase takes a duration of τ_c

Sensing information forwarding (SF) : Based on the echo signal received in the previous sub-phase, R forwards the information about the sensed process to MD using the remaining portion of harvested energy. This sub-phase lasts a duration of τ_e .

Moreover, this thesis assumes that the wireless channels between BS and R, R and MD are characterized by Rayleigh block fading for simplicity, with the same scale parameter of μ . The block time of ISAC-phase denoted by T is divided into three $\frac{T}{2}$ sub-blocks as detailed in Figure 3.2.

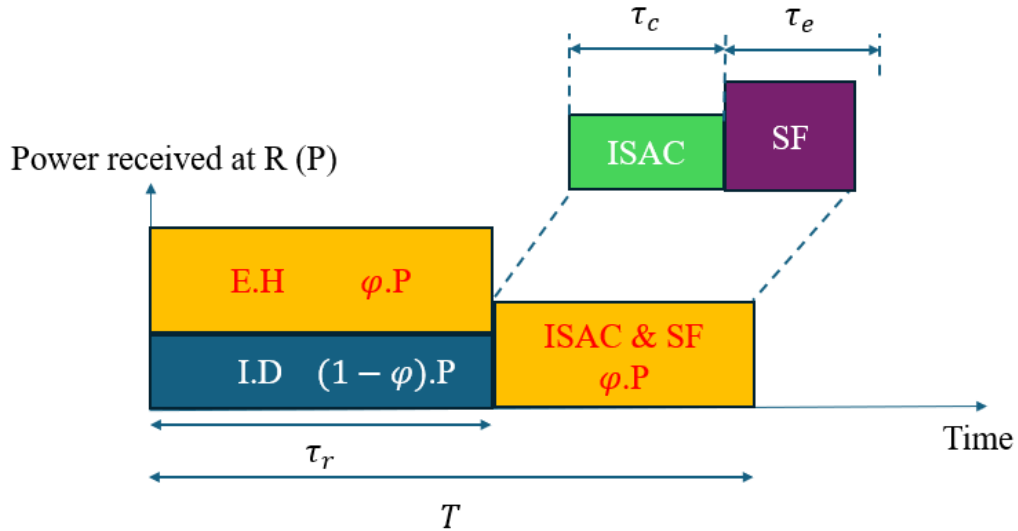


Figure 3.2 Power Splitting Relaying protocol at ISAC phase.

3.2 Phase I: SWIPT phase

In this phase, BS utilizes the same radio signal to send the source messages to R and to charge R concurrently [3].

3.2.1 Transmitter Model

Let $s(n)$ be the n -th symbols from the random zero-mean, unit variance source data signal s from the BS i.e., $\mathbb{E}[|s|^2] = 1$. $s(n)$, as shown in Figure 3.3, is first linear precoded

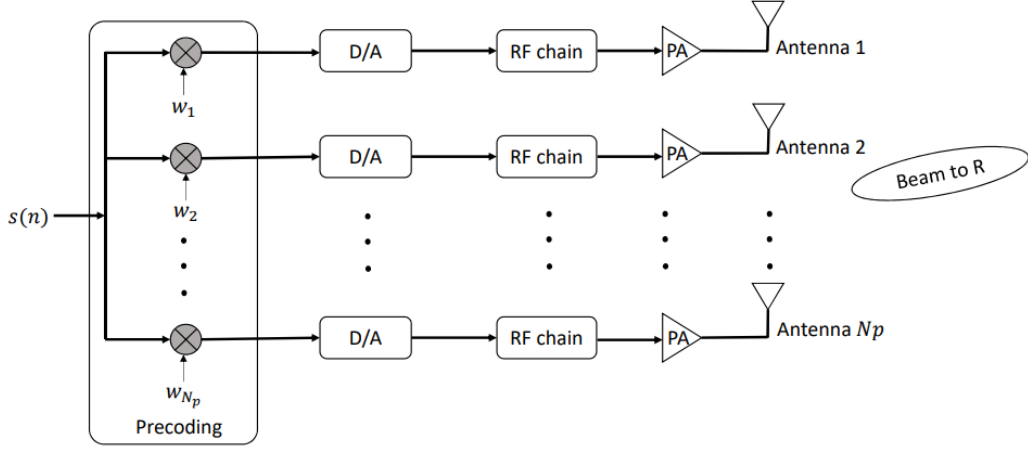


Figure 3.3 The illustration of the simplified transmit diversity model.

by a designed complex weight beamforming vector, which results in

$$\mathbf{x}_s(n) = \begin{bmatrix} w_1 \\ w_2 \\ \vdots \\ w_{N_p} \end{bmatrix} s(n) = \mathbf{w}s(n) \in \mathbb{C}^{N_p \times 1}, \quad (3.2)$$

where \mathbf{w} is the beamforming vector. Let the matrix $\mathbf{S} = \mathbb{E}[\mathbf{x}_s(n)\mathbf{x}_s^H(n)] = \mathbb{E}[\mathbf{w}(n)\mathbf{w}^H(n)]$ denote by the covariance matrix of the random baseband signal vector $\mathbf{x}(n)$. Then, the average power of the baseband signal is:

$$\mathbb{E}[\|\mathbf{x}_s(n)\|^2] = \text{tr}(\mathbf{S}) = \text{tr}(\mathbf{w}\mathbf{w}^H). \quad (3.3)$$

Each term $w_m s(n)$ ($m = 1, 2, \dots, N_p$) is sent to the m^{th} antenna to be modulated up to the RF band for transmission. After upconverting to RF band, the complex signal vector transmitted by BS is $\mathbf{x}_s(n, t) = \begin{bmatrix} x_1(n, t) \\ x_2(n, t) \\ \dots \\ x_{N_p}(n, t) \end{bmatrix} \in \mathbb{C}^{N_p \times 1}$ whose each element can be

expressed as

$$\begin{aligned} x_m(n, t) &= |w_m| s(n) \cos(\omega_c t + \phi_m) \\ &= \underbrace{\Re\{|w_m| e^{j\phi_m} e^{j\omega_c t}\}}_{w_m} s(n) \\ &= \Re\{w_m e^{j\omega_c t}\} s(n), \end{aligned}$$

where ω_c is the carrier angular frequency for all transmit antennas of BS, \tilde{w}_m and ϕ_m are the modulus and argument, respectively, of the complex weight beamforming w_m . The

average power of each transmitted signal denoted by P_m can be calculated as :

$$P_m = \frac{1}{T} \int_0^T x_m^2(n, t) dt = \frac{1}{2} |w_m s(n)|^2 = \frac{1}{2} |w_m|^2. \quad (3.4)$$

Here, if P is denoted by the overall power transmitted by the BS, I have a power constraint

$$\sum_{m=1}^{N_p} \frac{1}{2} |w_m|^2 \leq P. \quad (3.5)$$

Let denote by $\mathbf{w} \triangleq \begin{bmatrix} w_1 \\ w_2 \\ \dots \\ w_{N_p} \end{bmatrix} \in \mathbb{C}^{N_p \times 1}$, (3.5) can be rewritten as $\frac{1}{2} \|\mathbf{w}\|^2 = \frac{1}{2} \text{tr}(\mathbf{w}\mathbf{w}^H) \leq P$ or equivalent to $\text{tr}(\mathbf{S}) \leq 2P$.

3.2.2 Wireless channel

The RF signal received by R_X can be expressed as:

$$y_r(t) = \Re \{ \mathbf{h}_r^H \mathbf{w} s e^{j\omega_c t} \} + n_A(t), \quad (3.6)$$

where \mathbf{h}_r denotes the equivalent MISO complex channel coefficient vector between BS and R, while $n_A(t) = \Re \{ n_A e^{j\omega_c t} \}$ represents the thermal noise. Its baseband component n_A can be modeled as a complex Gaussian $\mathcal{CN}(0; \sigma_A^2)$ as explained in the reference [4].

3.3 Phase II: ISAC phase

This phase is split into three sub-phases. In the first sub-phase, R simultaneously implements energy harvesting and source information decoding based on the Power Splitting method. In the second one, R utilizes a portion of the harvested energy to do ISAC tasks. Specifically, R simultaneously senses the target object and forwards the decoded source information to MD. In the final sub-phase, R utilizes the remaining harvested energy to forward the sensing information to MD. Throughout the entire forwarding operation, R operates in the Decode-and-Forward (DF) mode.

3.3.1 Harvesting and Decoding

In this phase, from the received signal y_r from BS, R harvests a fraction of power denoted by ψ . The remaining fraction $(1 - \psi)$ is for source information decoding. Both workings take place simultaneously with the duration τ_r .

3.3.1.1 Energy Harvesting Architecture:

The energy harvesting process is first investigated, assuming that the noise's power is negligible. In this thesis, I used only the linear model for the energy harvesting (EH) process. With this model, the output power (DC) and input power of the EH circuit

are independent of each other. The output power is proportional to the input power with a constant conversion efficiency, whose values range from 0 to 1. An example of a rectenna, as presented in Fig. 3.4 typically comprises two main components: an antenna that collects RF signals from the air, and a single-diode rectifier that converts the collected signal to a DC signal. The antenna (R_X) is commonly modeled as an equivalent voltage source $v_s(t)$ in series with a source-resistor (antenna resistance) R_s . It, then,

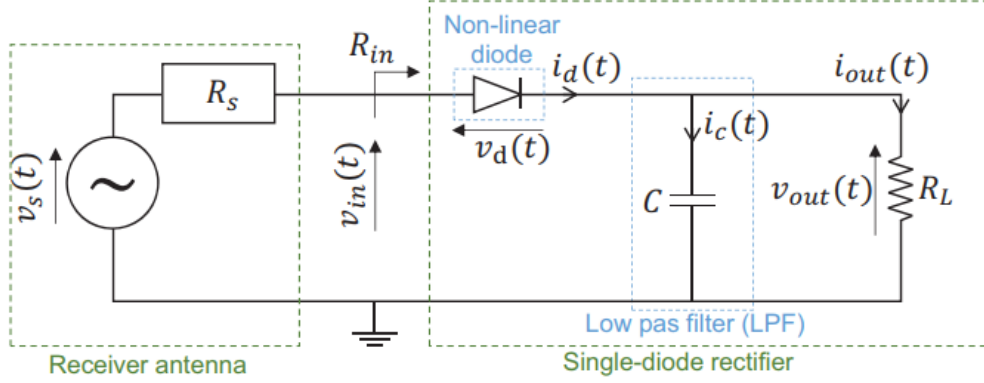


Figure 3.4 Rectenna equivalent circuit [3]

reflects the power transfer to the rectifier through the matching circuit. To maximize the transferred power, the matching circuit is typically well-tuned to the carrier frequency ω_c and is designed to match the input impedance (R_{in}) of the rectifier circuit. The rectifier is composed of a diode, which is non-linear, and a low-pass filter (LPF). The conversion efficiency η of the rectifier is defined as: $P_{out}^{DC} = \eta P_{in}^{RF}$, where P_{in}^{RF} is the power of the RF signal that enters the rectifier and P_{out}^{DC} is the converted output DC power. By assuming the linear EH model, the energy harvested per unit symbol time at R denoted by Q (in joule) is expressed as [54]:

$$Q = \eta \tau_r \mathbb{E} \left[|\mathbf{h}_r^H \mathbf{x}_s|^2 \right]. \quad (3.7)$$

3.3.1.2 Decoding Architecture:

The coherent demodulation process at R is illustrated in Figure 3.5 [4]. The baseband signal received at R_X can be written as

$$y_r = \mathbf{h}_r^H \mathbf{x}_s + n_A. \quad (3.8)$$

Then, I have the formula of SNR

$$\gamma_r = \frac{|\mathbf{h}_r^H \mathbf{x}_s|^2}{\sigma_A^2}. \quad (3.9)$$

3.3.1.3 Waveform design:

We aim to design the weight beamforming \mathbf{w} to maximize the harvested energy (EH)

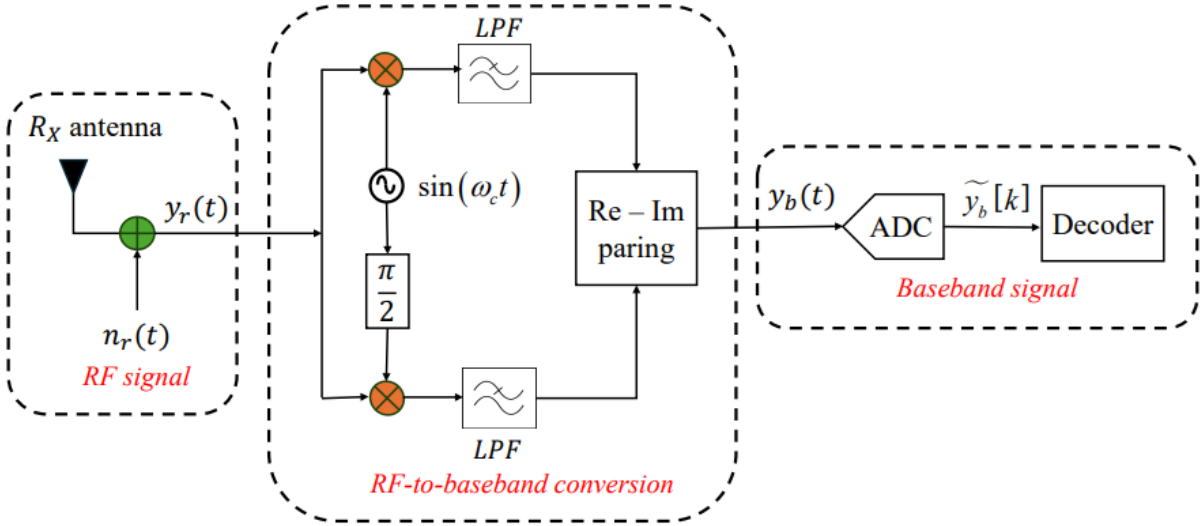


Figure 3.5 Coherent demodulation at R_X equivalent scheme [4]

and the achieved rate of source information decoding (ID).

Waveform design for Energy Harvesting:

$$\max_{\mathbf{w}} |\mathbf{h}_r^H \mathbf{w}|^2, \quad (3.10)$$

$$\text{subject to: } \|\mathbf{w}\|^2 \leq 2P. \quad (3.11)$$

Waveform design for information decoding:

$$\max_{\mathbf{w}} \text{SNR}, \quad (3.12)$$

$$\text{subject to: } \|\mathbf{w}\|^2 \leq 2P. \quad (3.13)$$

We can see that both the above optimization problems are the same. Both lead to the classic optimization problem of designing beamforming for MISO SNR subject to the power constraint, in this case, can be written as:

$$\max_{\mathbf{S}} \mathbf{h}_r^H \mathbf{S} \mathbf{h}_r \quad (3.14)$$

$$\text{subject to: } \text{tr}(\mathbf{S}) \leq 2P; \mathbf{S} \succeq 0. \quad (3.15)$$

With the pre-known MISO channel, the transmit strategy for the MISO channel would send the information only in the direction of the channel vector \mathbf{h}_r^H , and information sent in any remaining orthogonal direction will be nulled out by the channel anyway as in [23]. The optimum solution $\mathbf{S}^{opt} = 2P\mathbf{u}_1\mathbf{u}_1^H$, i.e., $\mathbf{w}^{opt} = \sqrt{2P}\mathbf{u}_1$ where $\mathbf{u}_1 = \frac{\mathbf{h}_r}{\|\mathbf{h}_r\|}$ is known as the Maximum Ratio Transmission (MRT) beamforming, at which, the beamformer using full overall power in the direction of channel vector \mathbf{h}_r^H as described in [54].

From this solution, the EH and SNR (in each individual case) can be written as:

$$Q = 2P\eta\tau_r\|\mathbf{h}_r\|^2; \gamma_r = \frac{2P}{\sigma_A^2}\|\mathbf{h}_r\|^2. \quad (3.16)$$

Note that, two optimized objectives are co-achievable if and only if the power of the received signal is totally harvested, while simultaneously the carried information is transmitted at a rate up to the MISO channel capacity. However, the two architectures (EH and ID) are quite different, i.e., existing EH circuits cannot directly decode the information in the RF-band signal. Therefore, I need some scheme at the receiver for an achievable rate-energy pair, the PS scheme as will be investigated in the following subsection is one such scheme.

3.3.1.4 Power-splitting method:

R applies PS to coordinate the processes of EH and ID from the received RF signal $y_r(t)$ as in Figure 3.6. More specifically, after the received signal is fed into the power splitter, the signal and the antenna noise are split to the information receiver and energy receiver separately. Then the power splitter splits the received signal in the power ratio denoted by $\rho : (1 - \rho)$. The portion $\sqrt{\rho}y_r(t)$ is sent to the EH architecture while the remaining signal strength, $\sqrt{1 - \rho}y_r(t)$ drives the ID architecture.

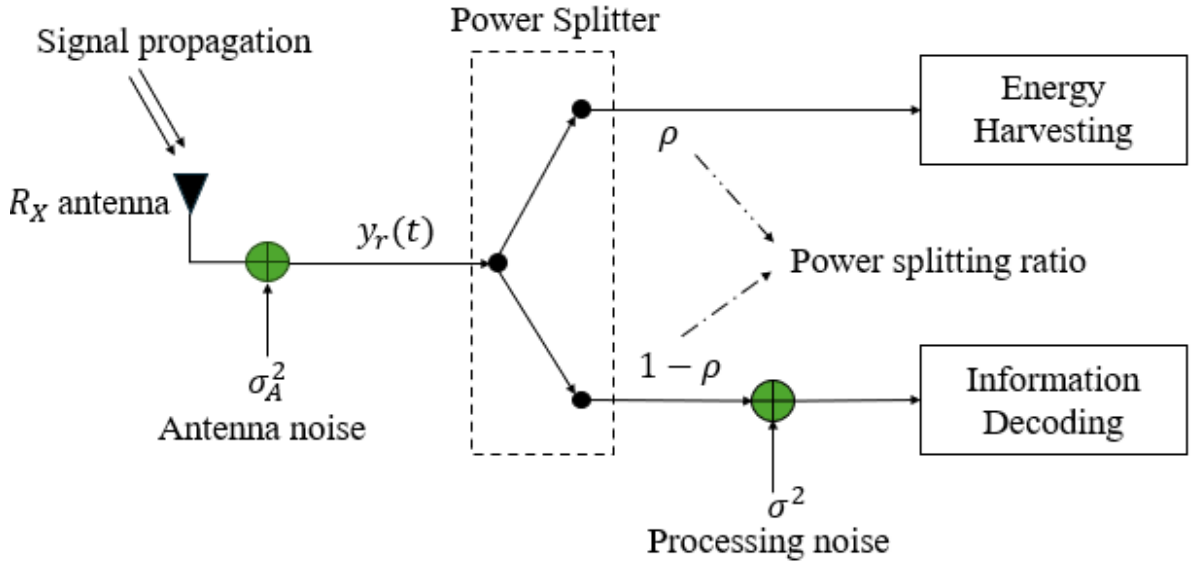


Figure 3.6 Power splitting scheme for receiver

The power splitter is assumed to be a perfect passive analog device; it does not introduce any extra power gain or noise, i.e. $0 \leq \rho \leq 1$. The information decoding circuit introduces an AWGN baseband processing noise $n_{ID} \sim \mathcal{CN}(0, \sigma^2)$ to the signal split to the information receiver. This noise can be assumed to be the noise due to quantization noise in the analog-to-digital (ADC) converter, it is independent of the antenna noise n_r , and as in the most practical wireless communication systems, it is assumed that the processing noise power is much greater than the antenna noise power, therefore the antenna

noise has negligible influence on both the ID and EH and can be omitted, as done in the works [55, 60, 61]. As a result, the signal split to the EH architecture of R is expressed as:

$$\sqrt{\rho}y_r(t) = \sqrt{\rho}\Re\{\mathbf{h}_r^H \mathbf{w} s e^{j\omega_c t}\}. \quad (3.17)$$

Then, the total harvested energy at R in the PS scheme is derived from the previous formula:

$$Q = \rho\eta\tau_r |\mathbf{h}_r^H \mathbf{w}|^2. \quad (3.18)$$

As a result, the transmit power at the relay for transmission in the next phases is depicted as:

$$P_r = \frac{Q}{T - \tau_r} = \frac{\tau_r}{T - \tau_r} \rho\eta |\mathbf{h}_r^H \mathbf{w}|^2. \quad (3.19)$$

Besides that, at the ID architecture, after splitting, the signal down conversion to base-band:

$$y_r = \sqrt{1 - \rho} \mathbf{h}_r^H \mathbf{x}_s + n_{ID}. \quad (3.20)$$

Accordingly, the SNR in the PS scheme is given similarly to the previous formula:

$$\gamma_r = \frac{(1 - \rho) |\mathbf{h}_r^H \mathbf{w}|^2}{\sigma^2}. \quad (3.21)$$

The optimal problem may differ from the previously discussed problems in this integrated EH and ID. case. To realize continuous information transfer, the SNR must be above a given target, denoted by γ_r^* . Meanwhile, the harvested power also needs to be large enough to maintain its operation. As some articles, with these constraints, the objective was to minimize the total transmission power [62, 63] or to maximize the energy harvested as in [64], or to maximize the achieved rate as in [54, 65], in this thesis, I given fixed the power splitting coefficient ρ , then, as described previous, the MRT beamforming $\mathbf{w} = \sqrt{2P} \frac{\mathbf{h}_r}{\|\mathbf{h}_r\|}$ is optimal for both energy harvesting and source information decoding. Therefore, by using the MRT beamforming, the harvested energy, the achieved rate, and the power available for transmission at the next phase after the PS process are:

$$Q = 2P\rho\eta\tau_r \|\mathbf{h}_r\|^2; \mathcal{R}_r = \frac{\tau_r}{T} \log_2(1 + \gamma_r); P_r = 2P\rho\eta \frac{\tau_r}{T - \tau_r} \|\mathbf{h}_r\|^2, \quad (3.22)$$

where the SNR of decoding at the relay is:

$$\gamma_r = \frac{2(1 - \rho)P}{\sigma^2} \|\mathbf{h}_r\|^2. \quad (3.23)$$

If I do not omit the effect of antenna noise, the SNR of decoding at the relay is:

$$\gamma_r = \frac{2(1 - \rho)P}{(1 - \rho)\sigma_A^2 + \sigma^2} \|\mathbf{h}_r\|^2.$$

3.3.2 ISAC task

In this sub-phase, treat the low-power devices as mono-static (the DoA/DoD are the same) dual-functional ISAC BS, i.e., transmit antenna T_X is shared for both radar sensing and communication, the communication signals can also be exploited as radar probing waveform [66]. R works in full-duplex mode, transmitting the dual-functional signal to MD and the target object surrounding environment while simultaneously receiving echoes from the target object.

By giving an amount of energy harvested previously, in this sub-phase, I will investigate the fundamental performance of the ISAC task system by analyzing both the communication performance and sensing performance. To do that, I assumed that the decoding is perfect in the previous, i.e. $s(n)$ is successfully recovered. In particular, I focus on the ISAC period consisting of L symbols. At R sends the discrete-time baseband dual-functional signal vector (the ISAC signal vector): $\mathbf{x}_I = [x_1, \dots, x_L]^T \in \mathbb{C}^{L \times 1}$, in which: x_i be the radar snapshot transmitted at i -th time slot with the perspective of sensing and be the i -th data symbol forwarding with the perspective of communication and L be the length of radar pulse/data frame.

The transmitting signal vector \mathbf{x}_I is defined by: $\mathbf{x}_I = \sqrt{\zeta P_r} \mathbf{s}_I^T$, where ζ is the portion of the harvested energy used for ISAC task, and $\mathbf{s}_I \in \mathbb{C}^{1 \times L}$ be the signaling data stream needs to be forwarded to MD with unit power, as introduced previously.

3.3.2.1 Communication Part:

By transmitting the signal \mathbf{x}_I the received signal at the MD is:

$$\mathbf{y}_c = h_c \mathbf{x}_I^T + \mathbf{z}_c^T = \sqrt{\zeta P_r} h_c \mathbf{s}_I + \mathbf{z}^T, \quad (3.24)$$

where h_c denotes the communication channel coefficient between MD and R with the assumption that it is modeled as a random channel with Rayleigh fading distribution and $\mathbf{z}_c \in \mathbb{C}^{L \times 1}$ denote the additive white Gaussian noise (AWGN) vector where each of its elements has the distribution of the form $\mathcal{CN}(0, \delta_c^2)$. From that, the achieved communication rate at MD with the duration τ_c is:

$$\mathcal{R}_c = \frac{\tau_c}{T} \log_2(1 + \gamma_c), \quad \text{where the SNR } \gamma_c = \frac{\zeta P_r |h_c|^2}{\delta_c^2}. \quad (3.25)$$

3.3.2.2 Sensing Part:

After transmitting the dual-functional signal for sensing the static target object surrounding environment, R receives back the reflected echo signal matrix, which can be expressed as follows [31], [32]:

$$\mathbf{y}_s = \mathbf{g} \mathbf{x}_I^T + \mathbf{z}_s^T, \quad (3.26)$$

where $\mathbf{g} \in \mathbb{C}^{M \times 1}$ denotes the target impulse response (TIR) vector where M denotes the number of complex fast-time samples (the number of range bins) with the echo signal

and $\mathbf{z}_s \in \mathbb{C}^{L \times M}$ denotes the noise vector where its components are assumed to be independently and identically distributed (i.i.d) and have the complex Gaussian distribution $\mathcal{CN}(0, \delta_s^2)$. Assuming the TIR vector can be modeled as a Gaussian random vector $\mathcal{CN}(\mathbf{0}, \mathbf{R})$, where \mathbf{R} defined by $\mathbf{R} = \mathbb{E}\{\mathbf{g}\mathbf{g}^H\} \in \mathbb{C}^{M \times M}$ is the full-rank (for simplicity) covariance/correlation matrix. Assuming that relay has access to \mathbf{R} , which assumption is used in the literature [67] and the references therein. The TIR is used to extract information about the target objects surrounding environment. For example, the reconstructed TIR can be modeled as the round-trip channel given by [68], [67], with the array of m range bins:

$$\mathbf{g} = \beta \mathbf{h}_s(r, \theta) \mathbf{h}_s^H(r, \theta), \quad (3.27)$$

where β is the complex amplitude (reflection coefficient) array proportional to the radar cross-sections (RCS) of the static target object located at the position specified by the DFRC transmitter's direction parameter r and θ , which are the distance and the angle from target respectively, $\mathbf{h}_s(r, \theta)$ is the far-field modeled coefficient channel vector between T_X and the target, which is the product of the channel gains and the location steering vector, which constructed from the location parameters as described in [69]. An example, by assuming the m -array of the range bin is uniform with the distance between two consecutively range bins is d , the location steering vector $\alpha(r, \theta)$ can be given as in [70, Chapter 6]: $\alpha(r, \theta) = \left[1, e^{-j\omega_c \frac{d \sin \theta}{c}}, \dots, e^{-j\omega_c (m-1) \frac{d \sin \theta}{c}}\right]^T$. Thus, in essence, sensing the target object is equivalent to estimating the interested target parameters to extracting environmental information based on \mathbf{g} from the received echo signal \mathbf{y}_s in equation (3.26), in which the transmitted signal is known by \mathbf{R} [67].

3.3.3 Sensing Information Forwarding

Based on the extracted information from the TIR \mathbf{g} of the sensing echo \mathbf{y}_s . Leveraging the remainder of harvested energy, the relay will send the sensed information symbol signal x_e for MD. Assuming that $\mathbb{E}[|x_e|^2] = 1$. The received signal at MD is expressed as:

$$y_e = \sqrt{(1 - \zeta)P_r} h_c x_e + z_e, \quad (3.28)$$

where z_e denoted the AWGN distributed as $\mathcal{CN}(0; \delta_e)$. Thus, I have the achieved rate during duration τ_e at MD is:

$$\mathcal{R}_e = \frac{\tau_e}{T} \log_2(1 + \gamma_e), \quad \text{where the SNR } \gamma_e = \frac{(1 - \zeta)P_r |h_c|^2}{\delta_e^2}. \quad (3.29)$$

3.4 Summary

This Chapter has described the proposed ISAC-assisted wireless systems model involving a Base Station (BS) communicating with a Mobile Device (MD) via a relay

(R) due to a poor direct link. The relay R, equipped with separate transmit and receive antennas, relays the BS signal to the MD and performs radar sensing, powered by energy harvested from the BS's signals. The system operates in two phases: the SWIPT phase for energy and signal transmission to R, and the ISAC phase for relaying and sensing. The details of performance analysis for each phase are present in the following.

CHAPTER 4. PERFORMANCE ANALYSIS

In this chapter, I will investigate the fundamental performance of the system, and finally, I will investigate the end-to-end outage event of the overall system. First, I will analyze the outage probability at the relay when decoding the source information and provide the exact formula for the outage probability at the relay. Next, I will analyze the performance of the ISAC system when aided by the relay. Specifically, for the communication part, I will analyze the outage probability at the MD when decoding the source forwarding signal from the relay. For the sensing part, I will analyze and present both the exact and asymptotic formulas for the sensing rate, as well as the CRLB estimation formula for distance. Finally, I will focus on analyzing and presenting the exact formula for the end-to-end outage probability of the entire system, including the relay forwarding the sensing information to the MD.

For the sake of analysis, I will introduce some self-defined constants and functions presented in Table 4.1 below, where three functions are the PDF of Gamma distribution, the CDF of Gamma distribution, and the CDF of exponential distribution respectively, from top to bottom.

Self-defined constants	Functions
$\kappa_r = \frac{\sigma^2}{2(1-\rho)P} \gamma_r^h$	$\Omega(x, \kappa, \theta) = \frac{1}{\theta^\kappa \Gamma(\kappa)} x^{\kappa-1} \exp\left(-\frac{x}{\theta}\right)$
$\kappa_c = \frac{\delta_c^2}{2\rho\xi\eta\frac{\tau_r}{T-\tau_r}P} \gamma_c^h$	$\Xi(x, \kappa, \theta) = 1 - \frac{\Gamma(\kappa, \frac{x}{\theta})}{\Gamma(\kappa)}$
$\kappa_e = \frac{\delta_e^2}{2\rho(1-\xi)\eta\frac{\tau_r}{T-\tau_r}P} \gamma_e^h$	$\Psi(x, \lambda) = 1 - \exp(-\lambda x)$

Table 4.1 Self-defined constants and functions.

4.1 Outage probability at Relay

The outage event is defined as the probability that the achievable rate is lower than a given target data rate. Given the data rate target for source decoding at R is \mathcal{R}_r^* . By definition, the outage probability (OP) of R for source decoding can be written as:

$$\mathcal{P}_r = \Pr(\mathcal{R}_r < \mathcal{R}_r^*) = \Pr\left(\gamma_r < 2^{\mathcal{R}_r^* \frac{T}{\tau_r}} - 1\right). \quad (4.30)$$

From the equation (3.23), after some algebraic manipulations, I obtain:

$$\mathcal{P}_r = \Pr \left(\|\mathbf{h}_r\|^2 < \frac{\sigma^2}{2(1-\rho)P} \gamma_r^* \right), \quad (4.31)$$

where $\gamma_r^* = 2^{\mathcal{R}_r^* \frac{T}{\tau_r}} - 1$, is known as the SNR threshold for source decoding at R.

Lemma 4.1. *Let $\mathbf{X} = (X_1, X_2, \dots, X_n)$ is a vector where each component is an independently Rayleigh distributed variable with the same scale parameter μ , then by the moment matching, the square norm of the vector is given by: $\|\mathbf{X}\|^2 = X_1^2 + X_2^2 + \dots + X_n^2$, will follow the Gamma distribution, $G(\kappa, \theta)$, with the shape parameter $\kappa = n$ and the scale parameter $\theta = 2\mu^2$. By that, the CDF of $\|\mathbf{X}\|^2$ will be written as the form:*

$$F_{\|\mathbf{X}\|^2}(x) = 1 - \frac{\Gamma(\kappa, \frac{x}{\theta})}{\Gamma(\kappa)} = 1 - \frac{\Gamma(n, \frac{x}{2\mu^2})}{\Gamma(n)},$$

where, $\Gamma(\kappa, x) = \int_x^\infty t^{\kappa-1} \exp(-t) dt$ and $\Gamma(n) = (n-1)!$ is the upper incomplete gamma function and the Gamma function respectively.

Assuming Rayleigh fading for the channel vector \mathbf{h}_r , where each component is i.ID with the same scale factor μ_r , then, by Lemma 4.1 the OP of R will have the exact form as:

$$\mathcal{P}_r = 1 - \frac{\Gamma\left(N_t, \frac{\sigma^2}{4(1-\rho)\mu_r^2 P} \gamma_r^*\right)}{\Gamma(N_t)}. \quad (4.32)$$

4.2 Performance in ISAC task

a) Performance of Communication

Outage Probability: Since the communication signal for MD is the source signal decoded and relayed by R, the outage event at MD will include the events: the rate is not achievable at R or the rate is achievable at R but not achievable at MD. Let \mathcal{R}_{rc}^{th} be the threshold rate to achieve at both R and MD, then the OP at MD can be formulated as:

$$\mathcal{P}_c = 1 - \Pr \left(\mathcal{R}_r > \mathcal{R}_{rc}^{th}, \mathcal{R}_c > \mathcal{R}_{rc}^{th} \right) = 1 - \Pr \left(\min \{ \mathcal{R}_r, \mathcal{R}_c \} > \mathcal{R}_{rc}^{th} \right), \quad (4.33)$$

Theorem 4.2. *The exact form of OP is given by:*

$$\mathcal{P}_c = 1 - \frac{\Gamma\left(N_t, \frac{\kappa_r}{2\mu_r^2}; \frac{\lambda_v \kappa_c}{2\mu_r^2}\right)}{\Gamma(N_t)}. \quad (4.34)$$

Proof. See the steps below to get the equation (4.66). □

b) Performance of Sensing

Sensing Rate: The sensing rate (SR) defines how much environmental information can be extracted per unit time, with the amount of information extracted also referred to as the sensing mutual information (MI) [67],[32]. The sensing MI is defined as the MI between the echo signal vector \mathbf{y}_s and the TIR \mathbf{g} with the given radar waveform \mathbf{x} . By assuming that each DFRC symbol lasts 1 unit time, I analyze SR through the sensing MI [67]:

$$\mathcal{R}_s = L^{-1} I(\mathbf{y}_s; \mathbf{g} | \mathbf{x}_I). \quad (4.35)$$

Reformulated the equation (3.26) into the vector form:

$$\text{vec}(\mathbf{y}_s^T) = \text{vec}(\mathbf{x}_I \mathbf{h}_s^T) + \text{vec}(\mathbf{z}_s). \quad (4.36)$$

Using the property compatibility with Kronecker product:

$$\text{vec}(\mathbf{u}\mathbf{v}) = (\mathbf{I}_m \otimes \mathbf{u}) \text{vec}(\mathbf{v}). \quad (4.37)$$

where $\mathbf{u}^{n \times 1}$ and $\mathbf{v}^{1 \times m}$ are column vector and row vector respectively, and denoted $\mathbf{Y} = \text{vec}(\mathbf{y}_s^T) \in \mathbb{C}^{LM \times 1}$, $\mathbf{Z} = \text{vec}(\mathbf{z}_s) \in \mathbb{C}^{LM \times 1}$, $\mathbf{X} = \mathbf{I}_M \otimes \mathbf{x}_I \in \mathbb{C}^{LM \times M}$, I can rewrite the above equation as the following complex classical linear model, similarly to [67], [25, Chapter 4]:

$$\mathbf{Y} = \mathbf{X}\mathbf{g} + \mathbf{Z}. \quad (4.38)$$

From this, the MI can be expressed as:

$$I(\mathbf{y}_s; \mathbf{g} | \mathbf{x}_I) = I(\mathbf{Y}; \mathbf{g} | \mathbf{X}) \quad (4.39)$$

$$= h(\mathbf{Y} | \mathbf{X}) - h(\mathbf{Y} | \mathbf{g}; \mathbf{X}) \quad (4.40)$$

$$= h(\mathbf{Y} | \mathbf{X}) - h(\mathbf{Z}), \quad (4.41)$$

in which the differential entropy and the conditional differential entropy are given by [71]:

$$h(\mathbf{X}) = - \int f(x) \log_2 f(x) dx, \quad (4.42)$$

$$h(\mathbf{X} | \mathbf{Y}) = - \int f(x, y) \log_2 f(x | y) dx dy, \quad (4.43)$$

where $f(x)$, $f(x, y)$, $f(x | y)$ denotes the PDF of the random vector (RV) \mathbf{X} , the joint PDF and the conditional PDF of \mathbf{X} given \mathbf{Y} of joint RVs (\mathbf{X}, \mathbf{Y}) respectively. The distribution of RV \mathbf{Y} in expression (4.38) is exploited to the distribution of linearity of standard Gaussian RV, so from explained in [72, Chapter 23], the RV \mathbf{Y} is a Gaussian vector

distributed as $\mathcal{CN}(\mathbf{0}; \mathbf{X}\mathbf{R}\mathbf{X}^H + \delta_s^2 \mathbf{I}_{LM})$.

Using (4.41), the MI is:

$$I(\mathbf{y}_s; \mathbf{g} | \mathbf{x}_I) = \log_2 [\det(\mathbf{X}\mathbf{R}\mathbf{X}^H + \delta_s^2 \mathbf{I}_{LM})] - \log_2 [\det(\delta_s^2 \mathbf{I}_{LM})] \quad (4.44)$$

$$= \log_2 [\det(\delta_s^{-2} \mathbf{X}\mathbf{R}\mathbf{X}^H + \mathbf{I}_{LM})] \quad (4.45)$$

$$= \log_2 [\det(\mathbf{I}_M + \delta_s^{-2} \mathbf{R}\mathbf{X}^H \mathbf{X})] \quad (4.46)$$

$$= \log_2 [\det(\mathbf{I}_M + \delta_s^{-2} \mathbf{x}^H \mathbf{x} \mathbf{R})] \quad (4.47)$$

$$= \log_2 [\det(\mathbf{I}_M + \delta_s^{-2} \zeta P_r L \mathbf{R})], \quad (4.48)$$

where (4.46) follows from the Sylvester's determinant identity: with $\mathbf{A}_{m \times n}$ and $\mathbf{B}_{n \times m}$:

$$\det(\mathbf{I}_m + \mathbf{A}\mathbf{B}) = \det(\mathbf{I}_n + \mathbf{B}\mathbf{A}). \quad (4.49)$$

From the result, I have the formula for the sensing rate:

$$\mathcal{R}_s = \frac{1}{L} \log_2 [\det(\mathbf{I}_M + \delta_s^{-2} \zeta P_r L \mathbf{R})]. \quad (4.50)$$

Using the eigendecomposition operation, the square matrix \mathbf{R} can be decomposed into:

$$\mathbf{R} = \mathbf{Q} \text{diag}(\lambda_1, \dots, \lambda_M) \mathbf{Q}^H, \quad (4.51)$$

where, \mathbf{Q} is a unitary matrix and $\text{diag}(\lambda_1, \dots, \lambda_M)$ is a diagonal matrix containing the eigenvalues $\lambda_1, \dots, \lambda_M$ of matrix \mathbf{R} . By applying Sylvester's determinant theorem once again, the sensing rate can be simplified to:

$$\mathcal{R}_s = \frac{1}{L} \log_2 [\det(\mathbf{I}_M + \delta_s^{-2} \zeta P_r L \text{diag}(\lambda_1, \dots, \lambda_M))] \quad (4.52)$$

$$= \frac{1}{L} \sum_{i=1}^r \log_2 (1 + \delta_s^{-2} \zeta P_r L \lambda_i), \quad (4.53)$$

where, r is the rank of matrix \mathbf{R} . When $P_r \rightarrow \infty$, I obtain the asymptotic form of the sensing rate as:

$$\mathcal{R}_s \approx \frac{1}{L} \sum_{i=1}^r \log_2 (\delta_s^{-2} \zeta P_r L \lambda_i) \quad (4.54)$$

$$= \frac{r}{L} \log_2 (\zeta P_r) + \frac{1}{L} \sum_{i=1}^r \log_2 (\delta_s^{-2} L \lambda_i). \quad (4.55)$$

CRLB estimation: To examine the estimation accuracy of the system, the CRLB is chosen as the performance metric which characterizes the lower bound on the variance (MSE) of any unbiased estimators [25]. In the scenario of rescue survivor, \mathbf{R} tends to estimate the unknown parameters of the target of interest, e.g. the range d from the target, the direction θ and reflection coefficient β of the target [73], the location of the

target [74], the velocity of the target [75],... In this thesis, I will use CRLB to analyze the estimation of the range d from a single target.

For a single target, when a radar signal pulse is transmitted, the round-trip time delay τ_0 from the transmitter to this target and echo back is related to the range d from the transmitter to the target as the formula: $\tau_0 = \frac{2d}{c}$, where c is the speed of propagation. Assuming that the propagation speed is given, the range estimation problem, therefore, is equivalent to the time delay estimation.

Consider the range estimation problem in radar sensing for this target. After transmitting a unit-power radar pulse $s_R(t)$ with bandwidth B and pulse duration T , the baseband echo radar signal at the input of the radar receiver can be modeled at the continuous waveform as follows:

$$y_R(t) = h_R \sqrt{P_{rad}} s_R(t - \tau_0) + n_A(t), \quad (4.56)$$

where h_R denotes the amplitude of the radar channel (combined antenna gain, radar cross-section, and path-loss propagation), $n_A(t)$ denotes the s circularly symmetric Gaussian noise with zero mean and variance σ_{noise}^2 at the sensing receiver, P_{rad} denotes the power radiation. The goal is to estimate the unknown real-valued parameter τ_0 by an estimator $\hat{\tau}_0$, which CRLB is attained. The CRLB of the variance of the delay estimator $\hat{\tau}_0$ is introduced as in [25, Chapter 3]

$$\text{Var}(\hat{\tau}_0) \geq CRLB_{\tau_0} = \frac{1}{8\pi^2 ISNR B_{rms}},$$

where $ISNR$ stands for integrated SNR and is defined by the ratio $\frac{|h_R|^2 T B P_{rad}}{\sigma_{noise}^2}$, $B_{rms} = \sqrt{\frac{\int_{-\infty}^{+\infty} f^2 |S(f)|^2 df}{\int_{-\infty}^{+\infty} |S(f)|^2 df}}$ is the root-mean-square (RMS) bandwidth of $s_R(t)$ with $S(f)$ is the Fourier transformation of transmitted baseband signal $s_R(t)$. From this, I can derive the CRLB for range estimation as below by using the parameter transformation estimate given in [25, Chapter 3]:

$$CRLB_d = \frac{c^2}{32\pi^2 ISNR B_{rms}}. \quad (4.57)$$

4.3 End-to-end outage performance

The outage event of the overall system will include additional cases, such as an outage in source information decoding at R. From the communication performance perspective, to prevent the entire system from experiencing an outage, then the minimum communication rate over all phases must be achievable at a specified rate. Let the end-to-end rate

is given by $\mathcal{R}_{\min} = \min \{\mathcal{R}_r, \mathcal{R}_c, \mathcal{R}_e\}$. By definition, the outage probability is given as:

$$\mathcal{P}_{\text{out}} = \Pr \left(\mathcal{R}_{\min} < \mathcal{R}_{rce}^{th} \right) = \Pr \left(\min \{\mathcal{R}_r, \mathcal{R}_c, \mathcal{R}_e\} < \mathcal{R}_{rce}^{th} \right) \quad (4.58)$$

$$= 1 - \Pr \left(\min \{\mathcal{R}_r, \mathcal{R}_c, \mathcal{R}_e\} > \mathcal{R}_{rce}^{th} \right) \quad (4.59)$$

$$= 1 - \Pr \left(\mathcal{R}_r > \mathcal{R}_{rce}^{th}, \mathcal{R}_c > \mathcal{R}_{rce}^{th}, \mathcal{R}_e > \mathcal{R}_{rce}^{th} \right) \quad (4.60)$$

$$= 1 - \Pr \left(\gamma_r > \gamma_r^{th}, \gamma_c > \gamma_c^{th}, \gamma_e > \gamma_e^{th} \right) \quad (4.61)$$

$$= 1 - \Pr(A, B, C). \quad (4.62)$$

where \mathcal{R}_{rce}^{th} being the target rate threshold required for all three subphases, $\gamma_m^{th} = (2^{\mathcal{R}_{rce}^{th} \frac{T}{\tau_m}} - 1)$ denoted the threshold SNRs of three-phases with $m \in \{r, c, e\}$, and A, B, C denoted individually the rate is achieved events of source decoding, source forwarding, and sensing forwarding respectively. I can see that the outage event of SF at MD is independent of the achieved rate being available or not for source forwarding at MD, i.e., regardless of whether γ_c is greater or less than γ_c^{th} . In other words, the events B and C are independent.

For the convenience of analysis, I denoted two random variables $U \triangleq \|\mathbf{h}_r\|^2$ and $V \triangleq |h_c|^2$. As described previously, U will follow the Gamma distribution as $G(N_t, 2\mu^2)$ and V follow exponential distributions with inverse scale parameters $\lambda_v = \mathbb{E}^{-1}[V] = \frac{1}{2\mu_c^2}$, respectively. The joint probability distribution at the e.q. (4.62) has been analyzed step-by-step in the following.

In general, the three-joint probability distribution in e.q (4.61) is exploited to the "lower-joint" probabilities in the events-form as: Due to the independence of events B and C, I can leverage this relationship to simplify the expression based on the conditional probability as follows:

$$\begin{aligned} \Pr(A, B, C) &= \Pr(A) \Pr(B, C|A) \\ &= \Pr(A) \Pr(B|A) \Pr(C|A) \\ &= \Pr(A) \frac{\Pr(A, B)}{\Pr(A)} \frac{\Pr(A, C)}{P(A)} \\ &= \frac{\Pr(A, B) \Pr(A, C)}{P(A)}. \end{aligned}$$

Building on this expansion, from the equation (4.61) I have:

$$\begin{aligned} \Pr(A, B, C) &= \frac{\Pr(\gamma_r > \gamma_r^{th}, \gamma_c > \gamma_c^{th}) \Pr(\gamma_r > \gamma_r^{th}, \gamma_e > \gamma_e^{th})}{\Pr(\gamma_r > \gamma_r^{th})} \\ &= \frac{\Pr(U > \kappa_r, UV > \kappa_c) \Pr(U > \kappa_r, UV > \kappa_e)}{\Pr(U > \kappa_r)}. \end{aligned}$$

The term at the denominator $\Pr(U > \kappa_r)$, can be expressed using the CDF of U , resulting in:

$$\Pr(U > \kappa_r) = 1 - \Xi(\kappa_r, N_t, 2\mu_r^2).$$

The two terms at the numerator have similar expressions, therefore, I only expand the first term here, with the remaining term expanded similarly. The first term, who is a joint probability $\Pr(U > \kappa_r, UV > \kappa_c)$, can be expressed as follows by using the CDFs and PDFs of U and V :

$$\begin{aligned} \Pr(U > \kappa_r, UV > \kappa_c) &= \Pr\left(U > \kappa_r, V > \frac{\kappa_c}{U}\right) \\ &= \int_{\kappa_r}^{\infty} \left[1 - F_V\left(\frac{\kappa_c}{U} \middle| U = u\right)\right] f_U(u) du, \end{aligned}$$

where:

$$f_U(u) = \Omega(u, N_t, 2\mu^2); \quad (4.63)$$

$$F_V(v) = \Psi(v, \lambda_v). \quad (4.64)$$

After some manipulation, I can get:

$$\Pr(U > \kappa_r, UV > \kappa_c) = \frac{1}{(2\mu_r^2)^{N_t} \Gamma(N_t)} \int_{\kappa_r}^{\infty} u^{N_t-1} \exp\left(\frac{-\lambda_v \kappa_c}{u} - \frac{u}{2\mu_r^2}\right) du. \quad (4.65)$$

By the Theorem 2, e.q. (13) in the article [76], I have the transform:

$$\int_x^{\infty} t^{\alpha-1} \exp\left(-at - \frac{b}{t}\right) dt = a^{-\alpha} \Gamma(\alpha, ax; ab), \quad a > 0,$$

where the Generalized incomplete Gamma function $\Gamma(\alpha, x; b)$ is defined from the equation (5) in [76]:

$$\Gamma(\alpha, x; b) = \int_x^{\infty} t^{\alpha-1} \exp\left(-t - \frac{b}{t}\right) dt.$$

Applying this the infinity integral in e.q (4.65) into the Generalized incomplete gamma function as:

$$\int_{\kappa_r}^{\infty} u^{N_t-1} \exp\left(\frac{-\lambda_v \kappa_c}{u} - \frac{u}{2\mu_r^2}\right) du = \left(\frac{1}{2\mu_r^2}\right)^{-N_t} \Gamma\left(N_t, \frac{\kappa_r}{2\mu_r^2}; \frac{\lambda_v \kappa_c}{2\mu_r^2}\right).$$

Resulting that, the first term will have the form:

$$\Pr(U > \kappa_r, UV > \kappa_c) = \frac{\Gamma\left(N_t, \frac{\kappa_r}{2\mu_r^2}; \frac{\lambda_v \kappa_c}{2\mu_r^2}\right)}{\Gamma(N_t)}. \quad (4.66)$$

Similarly, the remaining term at the numerator will have the form resulting:

$$\Pr(U > \kappa_r, UV > \kappa_e) = \frac{\Gamma\left(N_t, \frac{\kappa_r}{2\mu_r^2}, \frac{\lambda_v \kappa_e}{2\mu_r^2}\right)}{\Gamma(N_t)}. \quad (4.67)$$

Replace both the numerator and denominator I have:

$$\Pr(A, B, C) = \frac{1}{\Gamma(N_t)} \frac{\Gamma\left(N_t, \frac{\kappa_r}{2\mu_r^2}, \frac{\lambda_v \kappa_c}{2\mu_r^2}\right) \Gamma\left(N_t, \frac{\kappa_r}{2\mu_r^2}, \frac{\lambda_v \kappa_e}{2\mu_r^2}\right)}{\Gamma\left(N_t, \frac{\kappa_r}{2\mu_r^2}\right)}.$$

Finally, I have the exact form of the end-to-end OP as given by:

$$\mathcal{P}_{out} = 1 - \frac{1}{\Gamma(N_t)} \frac{\Gamma\left(N_t, \frac{\kappa_r}{2\mu_r^2}, \frac{\lambda_v \kappa_c}{2\mu_r^2}\right) \Gamma\left(N_t, \frac{\kappa_r}{2\mu_r^2}, \frac{\lambda_v \kappa_e}{2\mu_r^2}\right)}{\Gamma\left(N_t, \frac{\kappa_r}{2\mu_r^2}\right)}. \quad (4.68)$$

4.4 Summary

In this chapter, I perform a thorough analysis of the system's fundamental performance and end-to-end outage events, including relay-forwarded sensing information to the MD. The performance of the ISAC system with relay support, the outage probability at the MD for communication, and both exact and asymptotic formulas for the sensing rate and CRLB for range estimation are provided.

CHAPTER 5. NUMERICAL RESULTS AND DISCUSSIONS

This section presents representative numerical results to validate the developed analysis by illustrating the performance through both simulation and the previously established theory. In addition, I perform simulations of the sensing rate expression using two approaches: the exact approach and the asymptotic approach. The selected parameters are detailed below in Table 5.1. Several parameter values have been adopted from SWIPT and ISAC's existing articles [3, 7, 31, 32, 61, 74]. The main focus of this section is to compare the performance of Monte-Carlo simulations with the theoretical analysis. The simulation is carried out using 10^6 channel realizations. All graphs use transmitted power as the variable, specifically, in Figure 5.1, Figure 5.3, and Figure 5.4 use same three specific values of transmitted power 0 dBm, 5 dBm and 10 dBm. Figure 5.2, and Figure 5.5 use the same range of transmitted power values, from -10 dBm to 20 dBm.

Parameters	Value
Number of BS antenna, N_t	5 antennas
Bandwidth	10 MHz
Antenna noise power density, $\sigma_A^2 = \delta_c^2 = \delta_e^2$	-104 dBm/Hz
Information processing noise power density, σ^2	-70 dBm/Hz
Target data rate, $\mathcal{R}_r = \mathcal{R}_c = \mathcal{R}_e = \mathcal{R}_{rc} = \mathcal{R}_{rce}$	1 bit/s/Hz
Duration of each subphase, $\tau_r, \tau_c = \tau_e$	$\frac{T}{2}, \frac{T}{4}, \frac{T}{4}$, respectively
The distance between BS and R, d_{SR}	3 meters
The distance between R and MD, d_{RM}	7 meters
The distance between R and target object, d_{RT}	7 meters
Path-loss exponent factor, ε	4
Average signal power attenuation at reference distance, \mathcal{L}	-30 dBm
Power splitting ratio, ρ	0.3
Energy conversion efficiency of the EH process, η	0.7
The portion of energy harvesting used for ISAC, ξ	0.7
Length of Radar waveform, L	30
Number of range bins, M	4
Eigenvalues of the correlation matrix \mathbf{R} , $\{\lambda_i\}$	$\{1; 0.1; 0.05; 0.01\}$

Table 5.1 Simulation Parameters

The first of four figures below demonstrates the outage performance of communication, the final figure illustrates the sensing performance. As can be observed from

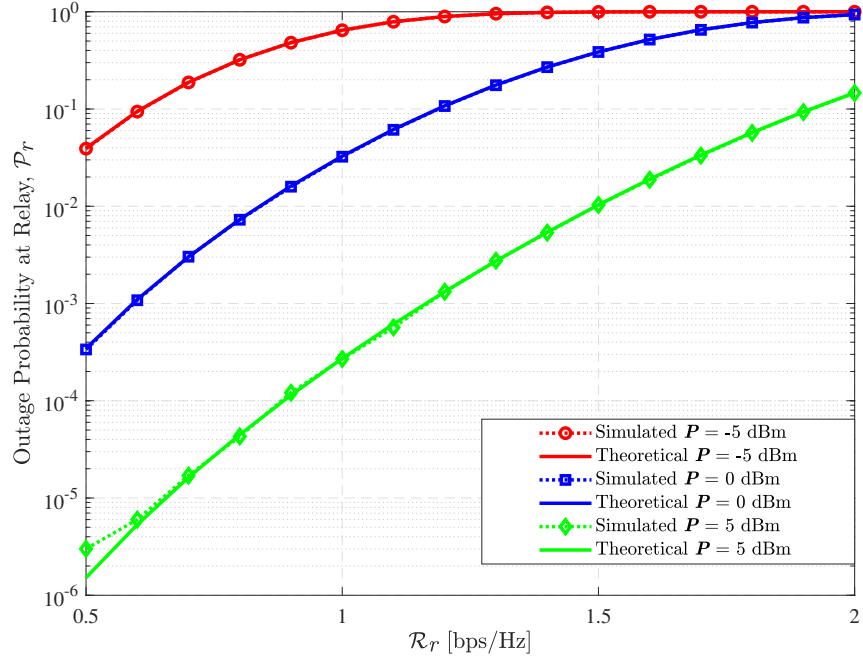


Figure 5.1 Outage probability at Relay, as a function of the transmit power at BS with fixed value $\rho = 0.3$.

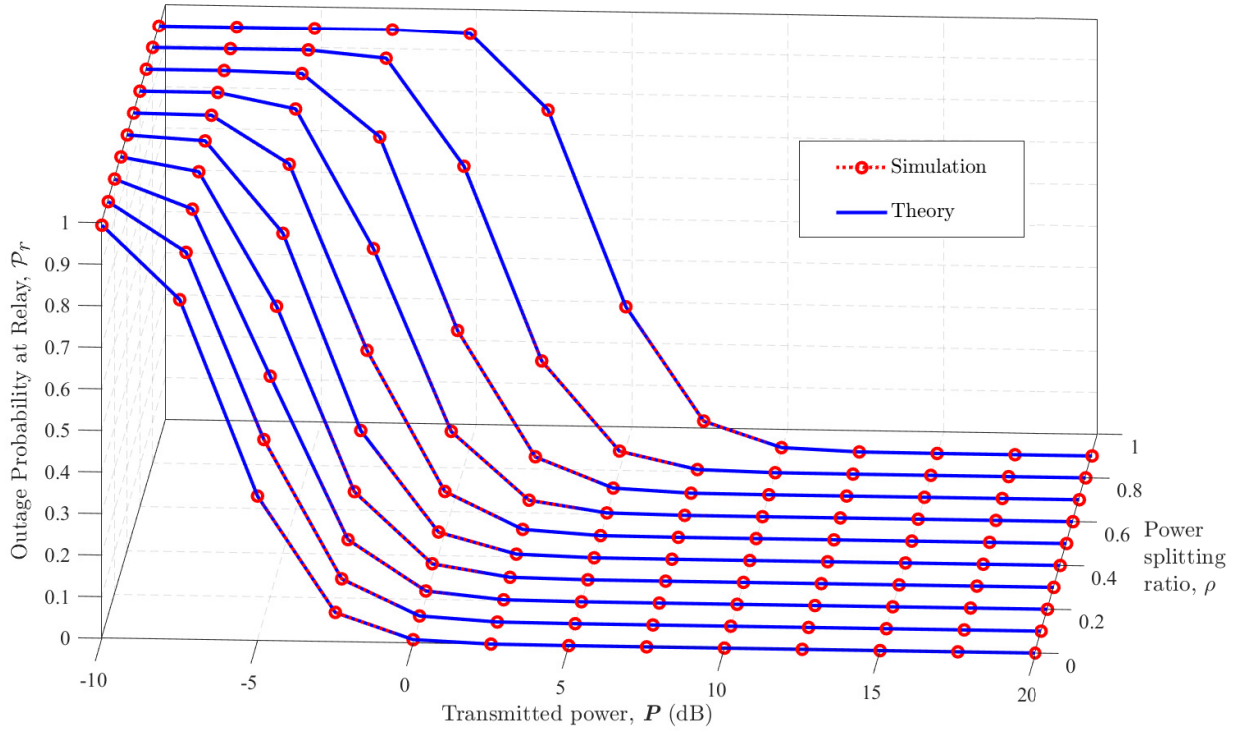


Figure 5.2 Outage probability at Relay as a function of the transmit power at BS and the power splitting ratio ρ .

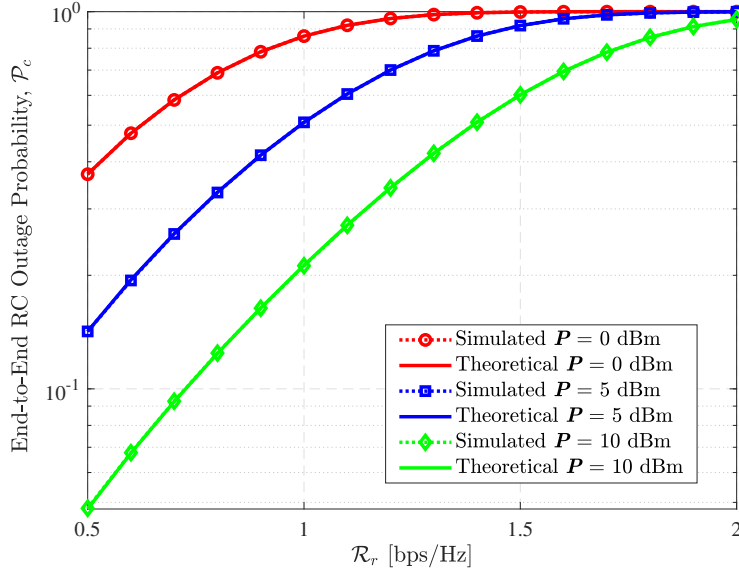


Figure 5.3 The outage probability for source information decoding at MD as a function of the transmit power at BS with fixed value $\rho = 0.3$.

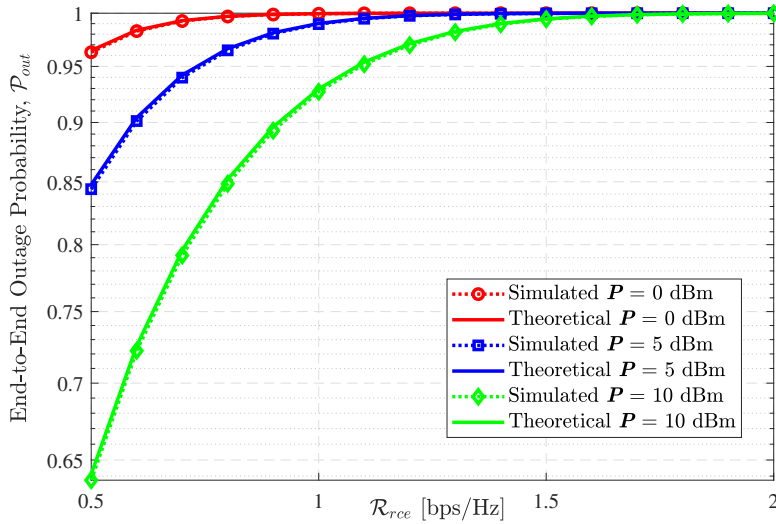


Figure 5.4 The end-to-end outage probability at MD as a function of the transmit power at BS with fixed value $\rho = 0.3$.

the first of four figures, the analytical results are well corroborated with the simulation results, which confirm the correctness of my developed analysis, as resulted in the equations (4.32), (4.34), (4.68). Specifically, figure 5.2 highlights the correctness of the theory formula by demonstrating the matching between the simulation and theoretical results across a range of transmitted power and power-splitting coefficient values. Also in this figure, we can see that for the same transmitted power value, the larger the ρ , the faster the outage probability at the relay converges to 1. Notably, when the transmitted

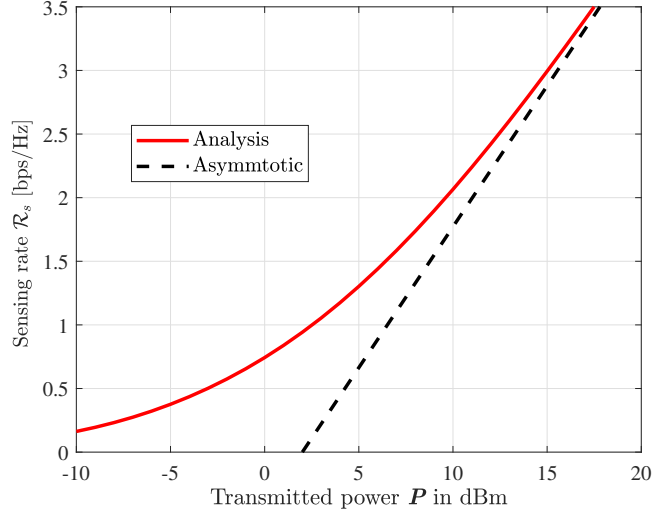


Figure 5.5 The sensing rate in ISAC task as a function of the transmit power at BS with fixed value $\rho = 0.3$

power starts to be less than 0, an ρ value of 0.5 or greater results in even higher outage occurrences, whereas, for values of ρ less than 0.5, the convergence of the outage probability to 1 is significantly slower. By observing Figure 5.1, we can see that with the fixed value of $\rho = 0.3$, the relay is still able to maintain source decoding at a reasonably acceptable level with a rate threshold of 1 bps/Hz when the transmit power is 0dBm, with the OP approximate $10^{-1.5}$. In three figures 5.1, 5.3. and 5.4, demonstrates that increasing the transmitted power and the rate threshold requirement will result in a smaller OP. Note that, because of the distance, even though in the same transmitted power, the OP at Relay in Figure 5.1 is always significantly lower compared to the OP in the two remaining figures. The end-to-end OP at figure 5.4 is highest among all. The reason is that the relay has to divide the harvested energy by the coefficient ξ between two sub-phases: ISAC task and sensing information forwarding, rather than using all harvested energy to serve each of them.

Figure 5.5 shows the sensing rate as a function of the transmit power P . From the equations (4.53) and (4.55), it is clear that the sensing rate is an increasing function of the transmitted power. Specifically, as shown in the graph, the sensing rate curve starts to rise sharply when the transmitter power exceeds 0dBm. The CRLB developed in the equation (4.57) is a decreasing function of transmitted power, so it will be smaller if the transmitted power is increased. The smaller the value of CRLB, the more accurate the distance estimation. In other words, the sensing performance improves as the transmit power increases. Furthermore, it can be seen from this graph that, the asymptotic results good track the provided simulation results accurately in the high transmitted power regime.

CONCLUSION

In this thesis, I conducted a comprehensive performance analysis of ISAC-assisted wireless systems with energy harvesting. Our investigation focused on evaluating the impact of integrating relay energy harvesting techniques into ISAC systems to enhance the efficiency and reliability of wireless communications and sensing tasks.

The key contributions of this thesis are as follows:

- **Proposal of a Relay Energy Harvesting Scheme:** I proposed a novel relay energy harvesting scheme specifically designed for ISAC systems. This scheme aims to improve both the efficiency and reliability of these systems, addressing a significant challenge in their deployment.
- **Comprehensive Performance Analysis:** I provided an in-depth performance analysis of the proposed system, examining critical metrics such as end-to-end outage probability and sensing rate. This analysis offers valuable insights into the system's capabilities and potential benefits.
- **Validation Through Numerical Results:** To support our analysis, I presented numerical results that validate the proposed scheme and demonstrate its practical advantages. These results highlight the effectiveness of the relay energy harvesting approach in enhancing ISAC system performance.

In summary, this thesis contributes to the field by offering a viable solution to the energy limitations of ISAC systems through the implementation of relay energy harvesting techniques. Our findings underscore the potential of this approach to significantly improve the operational efficiency and reliability of wireless communication and sensing applications, paving the way for more sustainable and robust IoT systems.

In the future, the main focus of our research will be on the actual deployment of the system, transitioning from theoretical analysis to practical implementation to further validate and optimize the proposed solutions.

REFERENCES

- [1] Z. Wei, H. Qu, Y. Wang, X. Yuan, H. Wu, Y. Du, K. Han, N. Zhang, and Z. Feng, “Integrated sensing and communication signals toward 5g-a and 6g: A survey,” *IEEE Internet of Things Journal*, vol. 10, no. 13, pp. 11068–11092, 2023.
- [2] A. Liu, Z. Huang, M. Li, Y. Wan, W. Li, T. X. Han, C. Liu, R. Du, D. K. P. Tan, J. Lu, *et al.*, “A survey on fundamental limits of integrated sensing and communication,” *IEEE Communications Surveys & Tutorials*, vol. 24, no. 2, pp. 994–1034, 2022.
- [3] B. Clerckx, R. Zhang, R. Schober, D. W. K. Ng, D. I. Kim, and H. V. Poor, “Fundamentals of wireless information and power transfer: From rf energy harvester models to signal and system designs,” *IEEE Journal on Selected Areas in Communications*, vol. 37, p. 4–33, Jan. 2019.
- [4] X. Zhou, R. Zhang, and C. K. Ho, “Wireless information and power transfer: Architecture design and rate-energy tradeoff,” in *2012 IEEE Global Communications Conference (GLOBECOM)*, IEEE, Dec. 2012.
- [5] Y. Li, F. Liu, Z. Du, W. Yuan, and C. Masouros, “Isac-enabled v2i networks based on 5g nr: How much can the overhead be reduced?,” in *2023 IEEE International Conference on Communications Workshops (ICC Workshops)*, pp. 691–696, IEEE, 2023.
- [6] R. Liu, M. Li, and A. L. Swindlehurst, “Joint beamforming and reflection design for ris-assisted isac systems,” in *2022 30th European Signal Processing Conference (EUSIPCO)*, pp. 997–1001, IEEE, 2022.
- [7] F. Liu, Y. Cui, C. Masouros, J. Xu, T. X. Han, Y. C. Eldar, and S. Buzzi, “Integrated sensing and communications: Toward dual-functional wireless networks for 6g and beyond,” *IEEE journal on selected areas in communications*, vol. 40, no. 6, pp. 1728–1767, 2022.
- [8] X. Cheng, D. Duan, S. Gao, and L. Yang, “Integrated sensing and communications (isac) for vehicular communication networks (vcn),” *IEEE Internet of Things Journal*, vol. 9, no. 23, pp. 23441–23451, 2022.
- [9] C. Ouyang, Y. Liu, and H. Yang, “Mimo-isac: Performance analysis and rate region characterization,” *IEEE Wireless Communications Letters*, vol. 12, no. 4, pp. 669–673, 2023.

- [10] Q. Liu, R. Luo, H. Liang, and Q. Liu, “Energy-efficient joint computation offloading and resource allocation strategy for isac-aided 6g v2x networks,” *IEEE Transactions on Green Communications and Networking*, vol. 7, no. 1, pp. 413–423, 2023.
- [11] Z. Behdad, Ö. T. Demir, K. W. Sung, and C. Cavdar, “Joint processing and transmission energy optimization for isac in cell-free massive mimo with urlhc,” *arXiv preprint arXiv:2401.10315*, 2024.
- [12] Y. Guo, C. Yin, O. Lu, M. Wang, and B. Xia, “Performance analysis for mm-wave isac systems with mutual benefit,” in *GLOBECOM 2022-2022 IEEE Global Communications Conference*, pp. 5438–5443, IEEE, 2022.
- [13] M. Liu, M. Yang, H. Li, K. Zeng, Z. Zhang, A. Nallanathan, G. Wang, and L. Hanzo, “Performance analysis and power allocation for cooperative isac networks,” *IEEE Internet of Things Journal*, vol. 10, no. 7, pp. 6336–6351, 2022.
- [14] H. Shoki, “Issues and initiatives for practical deployment of wireless power transfer technologies in japan,” *Proceedings of the IEEE*, vol. 101, no. 6, pp. 1312–1320, 2013.
- [15] Y. Chen, H. Hua, J. Xu, and D. W. K. Ng, “Isac meets swipt: Multi-functional wireless systems integrating sensing, communication, and powering,” *IEEE Transactions on Wireless Communications*, 2024.
- [16] X. Li, Z. Han, Z. Zhou, Q. Zhang, K. Huang, and Y. Gong, “Wirelessly powered integrated sensing and communication,” in *Proceedings of the 1st ACM MobiCom Workshop on Integrated Sensing and Communications Systems*, pp. 1–6, 2022.
- [17] H. Griffiths, L. Cohen, S. Watts, E. Mokole, C. Baker, M. Wicks, and S. Blunt, “Radar spectrum engineering and management: Technical and regulatory issues,” *Proceedings of the IEEE*, vol. 103, no. 1, pp. 85–102, 2014.
- [18] R. M. Mealey, “A method for calculating error probabilities in a radar communication system,” *IEEE Transactions on Space Electronics and Telemetry*, vol. 9, no. 2, pp. 37–42, 1963.
- [19] M. Roberton and E. Brown, “Integrated radar and communications based on chirped spread-spectrum techniques,” in *IEEE MTT-S International Microwave Symposium Digest, 2003*, vol. 1, pp. 611–614, IEEE, 2003.
- [20] Y. Cui, F. Liu, X. Jing, and J. Mu, “Integrating sensing and communications for ubiquitous iot: Applications, trends, and challenges,” *IEEE Network*, vol. 35, no. 5, pp. 158–167, 2021.

- [21] J. A. Zhang, F. Liu, C. Masouros, R. W. Heath, Z. Feng, L. Zheng, and A. Petropulu, "An overview of signal processing techniques for joint communication and radar sensing," *IEEE Journal of Selected Topics in Signal Processing*, vol. 15, no. 6, pp. 1295–1315, 2021.
- [22] F. Liu, Y.-F. Liu, A. Li, C. Masouros, and Y. C. Eldar, "Cramér-rao bound optimization for joint radar-communication beamforming," *IEEE Transactions on Signal Processing*, vol. 70, pp. 240–253, 2021.
- [23] D. Tse and P. Viswanath, *Fundamentals of Wireless Communication*. Cambridge University Press, May 2005.
- [24] A. Goldsmith, *Wireless communications*. Cambridge university press, 2005.
- [25] S. M. Kay, *Fundamentals of statistical signal processing: estimation theory*. Prentice-Hall, Inc., 1993.
- [26] Y. Ma, G. Zhou, and S. Wang, "Wifi sensing with channel state information: A survey," *ACM Computing Surveys (CSUR)*, vol. 52, no. 3, pp. 1–36, 2019.
- [27] S. M. Kay, "Statistical signal processing, volume ii, detection theory," 1998.
- [28] J. An, H. Li, D. W. K. Ng, and C. Yuen, "Fundamental detection probability vs. achievable rate tradeoff in integrated sensing and communication systems," *IEEE Transactions on Wireless Communications*, vol. 22, no. 12, pp. 9835–9853, 2023.
- [29] F. Dong, F. Liu, Y. Cui, W. Wang, K. Han, and Z. Wang, "Sensing as a service in 6g perceptive networks: A unified framework for isac resource allocation," *IEEE Transactions on Wireless Communications*, vol. 22, no. 5, pp. 3522–3536, 2022.
- [30] P. Tait, *Introduction to radar target recognition*, vol. 18. IET, 2005.
- [31] C. Ouyang, X. Zhang, and Y. Liu, "Performance analysis of downlink noma-isac," in *GLOBECOM 2023 - 2023 IEEE Global Communications Conference*, IEEE, Dec. 2023.
- [32] C. Ouyang, Y. Liu, and H. Yang, "Performance of downlink and uplink integrated sensing and communications (isac) systems," *IEEE Wireless Communications Letters*, vol. 11, p. 1850–1854, Sept. 2022.
- [33] C. Ouyang, Y. Liu, H. Yang, and N. Al-Dhahir, "Integrated sensing and communications: A mutual information-based framework," *IEEE Communications Magazine*, vol. 61, no. 5, pp. 26–32, 2023.

- [34] I. Krikidis, “Simultaneous information and energy transfer in large-scale networks with/without relaying,” *IEEE Transactions on Communications*, vol. 62, no. 3, pp. 900–912, 2014.
- [35] S. Bi, Y. Zeng, and R. Zhang, “Wireless powered communication networks: An overview,” *IEEE Wireless Communications*, vol. 23, no. 2, pp. 10–18, 2016.
- [36] E. C. Van Der Meulen, “Three-terminal communication channels,” *Advances in applied Probability*, vol. 3, no. 1, pp. 120–154, 1971.
- [37] M. Agiwal, A. Roy, and N. Saxena, “Next generation 5g wireless networks: A comprehensive survey,” *IEEE communications surveys & tutorials*, vol. 18, no. 3, pp. 1617–1655, 2016.
- [38] S. Efazati and P. Azmi, “Cross layer power allocation for selection relaying and incremental relaying protocols over single relay networks,” *IEEE Transactions on Wireless Communications*, vol. 15, no. 7, pp. 4598–4610, 2016.
- [39] J. N. Laneman, D. N. Tse, and G. W. Wornell, “Cooperative diversity in wireless networks: Efficient protocols and outage behavior,” *IEEE Transactions on Information theory*, vol. 50, no. 12, pp. 3062–3080, 2004.
- [40] Y. Hua, “An overview of beamforming and power allocation for mimo relays,” in *2010-MILCOM 2010 MILITARY COMMUNICATIONS CONFERENCE*, pp. 375–380, IEEE, 2010.
- [41] S. Agnihotri, S. Jaggi, and M. Chen, “Amplify-and-forward in wireless relay networks,” in *2011 IEEE Information Theory Workshop*, pp. 311–315, IEEE, 2011.
- [42] A. H. Mohammed, B. Dai, B. Huang, M. Azhar, G. Xu, P. Qin, and S. Yu, “A survey and tutorial of wireless relay network protocols based on network coding,” *Journal of Network and Computer Applications*, vol. 36, no. 2, pp. 593–610, 2013.
- [43] T. Cover and A. E. Gamal, “Capacity theorems for the relay channel,” *IEEE Transactions on information theory*, vol. 25, no. 5, pp. 572–584, 1979.
- [44] E. Antonio-Rodríguez, R. López-Valcarce, T. Riihonen, S. Werner, and R. Wichman, “Adaptive self-interference cancellation in wideband full-duplex decode-and-forward mimo relays,” in *2013 IEEE 14th workshop on signal processing advances in wireless communications (SPAWC)*, pp. 370–374, IEEE, 2013.
- [45] Y. Liu, W. Xu, K. Niu, Z. He, and B. Tian, “A practical compress-and-forward relay scheme based on superposition coding,” in *2012 IEEE 14th International Conference on Communication Technology*, pp. 1286–1290, IEEE, 2012.

- [46] S.-H. Lee and S.-Y. Chung, “When is compress-and-forward optimal?,” in *2010 Information Theory and Applications Workshop (ITA)*, pp. 1–3, IEEE, 2010.
- [47] R. Shankar, G. Kumar, V. Sachan, and R. Mishra, “An investigation of two phase multi-relay s-df cooperative wireless network over time-variant fading channels with incorrect csi,” *Procedia Computer Science*, vol. 125, pp. 871–879, 2018.
- [48] S. S. Ikki and M. H. Ahmed, “Performance analysis of incremental-relaying cooperative-diversity networks over rayleigh fading channels,” *IET communications*, vol. 5, no. 3, pp. 337–349, 2011.
- [49] A. Hadjtaieb, A. Chelli, M.-S. Alouini, and H. Boujemaa, “Performance analysis of selective decode-and-forward multinode incremental relaying with maximal ratio combining,” in *Fourth International Conference on Communications and Networking, ComNet-2014*, pp. 1–6, IEEE, 2014.
- [50] M. Zimmer, A. Holzhausen, and A. Parmar, “More emissions than meet the eye: Decarbonizing the ict sector,” *Westminster, CA, USA: Allianz Research*, 2023.
- [51] D. Wang, R. Zhang, X. Cheng, and L. Yang, “Relay selection in power splitting based energy-harvesting half-duplex relay networks,” in *2017 IEEE 85th Vehicular Technology Conference (VTC Spring)*, pp. 1–5, IEEE, 2017.
- [52] L. R. Varshney, “Transporting information and energy simultaneously,” in *2008 IEEE International Symposium on Information Theory*, pp. 1612–1616, 2008.
- [53] U. Raza and A. Salam, “On-site and external energy harvesting in underground wireless,” *Electronics*, vol. 9, no. 4, p. 681, 2020.
- [54] R. Zhang and C. K. Ho, “Mimo broadcasting for simultaneous wireless information and power transfer,” *IEEE Transactions on Wireless Communications*, vol. 12, p. 1989–2001, May 2013.
- [55] D. W. K. Ng, E. S. Lo, and R. Schober, “Robust beamforming for secure communication in systems with wireless information and power transfer,” *IEEE Transactions on Wireless Communications*, vol. 13, no. 8, pp. 4599–4615, 2014.
- [56] I. Krikidis, S. Sasaki, S. Timotheou, and Z. Ding, “A low complexity antenna switching for joint wireless information and energy transfer in mimo relay channels,” *IEEE Transactions on Communications*, vol. 62, no. 5, pp. 1577–1587, 2014.
- [57] H. Jayakumar, K. Lee, W. S. Lee, A. Raha, Y. Kim, and V. Raghunathan, “Powering the internet of things,” in *Proceedings of the 2014 international symposium on Low power electronics and design*, pp. 375–380, 2014.

- [58] A. A. Nasir, X. Zhou, S. Durrani, and R. A. Kennedy, "Wireless-powered relays in cooperative communications: Time-switching relaying protocols and throughput analysis," *IEEE Transactions on Communications*, vol. 63, no. 5, pp. 1607–1622, 2015.
- [59] X. Di, K. Xiong, P. Fan, and H.-C. Yang, "Simultaneous wireless information and power transfer in cooperative relay networks with rateless codes," *IEEE Transactions on Vehicular Technology*, vol. 66, no. 4, pp. 2981–2996, 2016.
- [60] L. Liu, R. Zhang, and K.-C. Chua, "Wireless information and power transfer: A dynamic power splitting approach," *IEEE Transactions on Communications*, vol. 61, no. 9, pp. 3990–4001, 2013.
- [61] G. Pan, H. Lei, Y. Yuan, and Z. Ding, "Performance analysis and optimization for swipt wireless sensor networks," *IEEE Transactions on Communications*, vol. 65, no. 5, pp. 2291–2302, 2017.
- [62] S. Timotheou, I. Krikidis, G. Zheng, and B. Ottersten, "Beamforming for miso interference channels with qos and rf energy transfer," *IEEE Transactions on Wireless Communications*, vol. 13, no. 5, pp. 2646–2658, 2014.
- [63] Q. Shi, L. Liu, W. Xu, and R. Zhang, "Joint transmit beamforming and receive power splitting for miso swipt systems," *IEEE Transactions on Wireless Communications*, vol. 13, no. 6, pp. 3269–3280, 2014.
- [64] J. Xu, L. Liu, and R. Zhang, "Multiuser miso beamforming for simultaneous wireless information and power transfer," *IEEE Transactions on Signal Processing*, vol. 62, no. 18, pp. 4798–4810, 2014.
- [65] K. Huang and E. Larsson, "Simultaneous information and power transfer for broadband wireless systems," *IEEE Transactions on Signal Processing*, vol. 61, no. 23, pp. 5972–5986, 2013.
- [66] F. Liu, C. Masouros, A. Li, H. Sun, and L. Hanzo, "Mu-mimo communications with mimo radar: From co-existence to joint transmission," *IEEE Transactions on Wireless Communications*, vol. 17, p. 2755–2770, Apr. 2018.
- [67] B. Tang and J. Li, "Spectrally constrained mimo radar waveform design based on mutual information," *IEEE Transactions on Signal Processing*, vol. 67, p. 821–834, Feb. 2019.
- [68] J. Li and P. Stoica, "Mimo radar with colocated antennas," *IEEE Signal Processing Magazine*, vol. 24, p. 106–114, Sept. 2007.

- [69] Y. Liu, Z. Wang, J. Xu, C. Ouyang, X. Mu, and R. Schober, “Near-field communications: A tutorial review,” *IEEE Open Journal of the Communications Society*, 2023.
- [70] P. Stoica and R. Moses, “Spectral analysis of signals,” *Prentice Hall*, 01 2005.
- [71] T. M. Cover and J. A. Thomas, *Elements of Information Theory (Wiley Series in Telecommunications and Signal Processing)*. USA: Wiley-Interscience, 2006.
- [72] A. Lapidoth, *A foundation in digital communication*. Cambridge University Press, 2017.
- [73] I. Bekkerman and J. Tabrikian, “Target detection and localization using mimo radars and sonars,” *IEEE Transactions on Signal Processing*, vol. 54, p. 3873–3883, Oct. 2006.
- [74] K. Meng and C. Masouros, “Cooperative sensing and communication for isac networks: Performance analysis and optimization,” *arXiv preprint arXiv:2403.20228*, 2024.
- [75] P. Kumari, J. Choi, N. González-Prelcic, and R. W. Heath, “Ieee 802.11 ad-based radar: An approach to joint vehicular communication-radar system,” *IEEE Transactions on Vehicular Technology*, vol. 67, no. 4, pp. 3012–3027, 2017.
- [76] M. Chaudhry and S. Zubair, “Generalized incomplete gamma functions with applications,” *Journal of Computational and Applied Mathematics*, vol. 55, p. 99–124, Oct. 1994.